AD-A268 697

THERMAL INSULATION OF
WET SHIELDED METAL ARC WELDS

by

PATRICK JOSEPH KEENAN

B.A. Chemistry, 1982
University of Pennsylvania, Philadelphia, Pennsylvania

Submitted to the Departments of
Ocean Engineering, and Materials Science and Engineering
in Partial Fulfillment of the Requirements for the Degrees of

NAVAL ENGINEER
and
MASTER OF SCIENCE IN MATERIALS ENGINEERING

at the
Massachusetts Institute of Technology
June 1993

DTIC
ELECTE
AUG 3 1 1993
S B D

Signature of Author _____
Department of Ocean Engineering
7 May 1993

Certified by _____
Koichi Masubuchi
Kawasaki Professor of Engineering
Department of Ocean Engineering, Thesis Supervisor
Department of Materials Science and Engineering, Thesis Supervisor

Accepted by _____
Linn W. Hobbs
John F. Elliot Professor of Materials
Chair, Departmental Committe on Graduate Students

Accepted by _____
Professor A. Douglas Carmichael
Chairman, Department Graduate Committee
Department of Ocean Engineering

0 3 6

93-20136

THERMAL INSULATION OF
WET SHIELDED METAL ARC WELDS

by

Patrick Joseph Keenan

Submitted to the Departments of Materials Science and Engineering and Ocean
Engineering on May 7, 1993 in partial fulfillment of the requirements for the degrees of
Master of Science in Materials Engineering and Naval Engineer

ABSTRACT

Computational and experimental studies were performed to determine the effect of static
thermal insulation on the quality of wet shielded metal arc welds (SMAW). A
commercially available heat flow and fluid dynamics spectral-element computer program
was used to model a wet SMAW and to determine the potential effect on the weld
cooling rate of placing thermal insulation adjacent to the weld line. Experimental manual
welds were made on a low carbon equivalent (0.285) "mild steel" and on a higher carbon
equivalent (0.410) "high tensile strength" steel, using woven fabrics of alumina-boria-
silica fibers to insulate the surface of the plate being welded. The effect of the insulation
on weld quality was evaluated through the use of post-weld Rockwell Scale hardness
measurements on the surface of the weld heat affected zones (HAZs) and by visual
inspection of sectioned welds at 10 X magnification.

The computational simulation demonstrated a 150% increase in surface HAZ peak
temperature and a significant decrease in weld cooling rate with respect to uninsulated
welds, for welds in which ideal insulation had been placed on the base plate surface
adjacent to the weld line. Experimental mild steel welds showed a reduction in surface
HAZ hardness attributable to insulation at a 77% significance level. A visual comparison
of the cross-sections of two welds made in 0.410 carbon equivalent steel—with
approximately equivalent heat input—revealed underbead cracking in the uninsulated
weld but not in the insulated weld.

This work has lead to the filing of a patent through the Technology Licensing Office of
the Massachusetts Institute of Technology and to the initiation of a developmental
research project by the Underwater Ship Husbandry branch of the United States Naval
Sea Systems Command.

Thesis Supervisor: Koichi Masubuchi
      Title: Professor of Ocean Engineering and Material Science and Engineering

ACKNOWLEDGMENTS

I wish to thank the following people for the assistance that they provided during the course of my research.

Mr. Robert Murray of the Naval Sea Systems Command for his logistic support of my experimental work.

Mr. Gokhan Goktug of MIT who helped me set up the experiment, and patiently recorded experimental parameters while I welded.

My thesis advisor, Professor Masubuchi, for being constantly available to offer guidance and advice.

Finally, my wife, Jean M. Fiore, for her patience and editorial skills, both of which I relied on heavily during the preparation of this manuscript.

TABLE OF CONTENTS

5

LIST OF TABLES

LIST OF FIGURES

7

CHAPTER 1. INTRODUCTION

Underwater welding processes are classified as dry or wet based on exposure to the ambient environment. Processes that are physically protected from the surrounding water are classified as dry, whereas wet welding processes are those in which the weld is directly exposed to the underwater environment.

Four dry welding processes are currently in use [1]:

• One-Atmosphere Welding. One-atmosphere welding is performed in a pressure vessel at approximately one atmosphere absolute. Welders who are not trained divers can perform this type of welding after being transferred to the pressure vessel.

• Habitat Welding. Welding performed in open-bottom chambers by divers who have removed their diving equipment is classified as habitat welding. In both one-atmosphere and habitat welding, a complete atmosphere conditioning system must be used in conjunction with the chamber or habitat. Welding and respiratory exhaust gases must be vented, and breathing gas supplied to the artificial environment.

• Dry Chamber Welding. Dry chamber welding is performed by a diver in diving equipment in an open-bottom enclosure. Full atmosphere conditioning systems are not required for dry chamber welding since breathing gases are supplied via the diving equipment. However, diver and welding exhaust gases must be vented from these chambers to prevent explosions and loss of chamber seal from over-pressurization. Gas metal arc (GMA), gas tungsten arc (GTA), and shielded metal arc (SMA) processes can be used in dry chambers as well as in one-atmosphere pressure vessels and habitats. Electrical resistance pre- and post-heating can also be used in these environments.

• Dry Spot Welding. Dry spot welding is a process in which water is displaced from the local weld area by a transparent gas-filled box or via shielding gas surrounded by a concentric ring of water jets. Divers move the dry box or water-jet welding apparatus along the joint as the weld is made. Dry box welding is inherently suited to the gas metal arc welding (GMAW) process because the filler wire can be fed continuously through the center of the gas box or water-jet to the weld. Welds made with the dry spot process cannot be pre- or post-heated because the only section of these welds that is isolated from the water is the area adjacent to the arc.

In the case of wet welding, the only viable process for making linear joints that has been developed to date is shielded metal arc welding (SMAW). (Friction stud welding has been used with considerable success to make wet *spot* welds). In wet SMAW, an arc is struck in the water between an electrode and the surface being welded.

Divers move the electrode along the weld line. No active thermal treatment of wet welds is feasible because of their direct exposure to the underwater environment.

1.1 Comparison of Wet and Dry Underwater Welding Processes

Wet welding is generally faster and less expensive than dry underwater welding. The former can be performed on structures of any shape and in confined areas. The pressure vessels, habitats and cofferdams required for most dry underwater welding procedures may be difficult or impossible to install on geometrically complex structures or in physically restricted areas. Fabrication and installation of these enclosures is time consuming and expensive. Dry spot welding equipment is also more expensive than the equipment required for wet SMAW. Thus, wet welding is suited for quick inexpensive repairs.

Wet welding is not as versatile as dry underwater welding with respect to the variety of processes that can be performed (i.e., GMAW, GTAW, SMAW). However, since most underwater structures are built with relatively thick material and diver or remotely operated vehicle (ROV) time at depth is expensive, high deposition rate processes are required for underwater welding. Therefore, even in enclosures where GMAW and GTAW could be used, SMAW is the most frequently used welding process.

The primary disadvantage of wet SMAW is that direct exposure to water deleteriously affects weld quality and limits the types of materials that can be joined.

1.2 Applications of Underwater Welding Procedures

Currently, critical welds such as joints in primary strength members of offshore structures, pressurized pipeline joints, and hull integrity seams on ships and submarines are made with dry underwater procedures. Quality cannot be compromised in these applications so wet SMAW cannot be used. Additionally, welding of high yield strength steels must be accomplished with dry procedures irrespective of the joint application. No wet SMAW process has been developed that will produce satisfactory joints in these materials. Wet SMAW is used only for non-critical or temporary joints in mild steel structures. Industrial use of wet SMAW is found in secondary structural member joints on offshore platforms, installation of temporary patches and lifting points in marine salvage, and construction and repair of coastal zone structures (i.e., piers and breakwaters).

Underwater welding is commonly employed in the commercial and military sectors of the maritime industry. Oceaneering Inc., a company that performs contracted underwater repair services on offshore petroleum and natural gas platforms and pipelines,

9

and on ships, billed customers for approximately 5 million dollars of underwater welding services in fiscal year 1992.

The U.S. Navy spent 3.3 million dollars on underwater weld repairs over the 1989-92 period. Fifty percent of these expenditures were for wet welds. Because of their poor quality, the Navy has classified all wet welds as temporary repairs with the exception of one non-critical application: the sealing of hull openings in ships that are being de-commissioned. Consequently, all wet welds made on active Navy ships and submarines must eventually be removed and replaced by either dry underwater welds or welds made in drydock.

The expense incurred as a result of reworking temporary wet welds is significant. Drydocking costs for naval surface combatants range from approximately 250,000 to 1.5 million fiscal year 1992 dollars ($ FY '92). Submarine drydocking costs are on the order of 1 million $ FY '92. These are costs only for docking and undocking the vessel, and do not include direct or indirect costs of the repair work. Additionally, drydocking vessels for replacement of temporary weld repairs disrupts fleet employment and maintenance schedules.

An advance in technology that improved the quality and scope of wet SMA welds so that permanent wet welds could be used in more critical applications and on more materials could provide substantial cost savings to industry and the military.

CHAPTER 2. BACKGROUND

The primary construction material used in the marine environment is steel. Consequently, only welding of steel will be considered in this thesis. Several processes have been developed for welding steel in a dry environment: GMAW, GTAW, SMAW and submerged arc welding. Because of their relatively low metal deposition rates for manual welding, and the difficulty of displacing water with pressurized shielding gases, GMAW and GTAW are not suited for wet underwater welding. Submerged arc welding offers a high deposition rate but covering a joint—even with a hydrophobic flux, if one could be developed—and maintaining joint coverage in a moving fluid environment would be difficult, especially when most joints made underwater are either in vertical or overhead positions. Therefore, wet welding is currently performed almost exclusively using the SMAW process. The equipment and procedures used for wet SMAW are quite similar to those used for SMAW in air. The most significant difference is that specialized electrodes have been developed for wet SMAW. Additionally, power supplies for underwater SMAW must be capable of moving sufficient current through the relatively long welding leads that are required because of the separation of the power source from the submerged work-site.

2.1 Technical Problems Associated With Wet SMA Welds

Wet SMA welding arcs are protected from the surrounding water by a bubble of gas produced by the decomposition of the electrode flux. The flux heat of vaporization is provided by resistive heating of the electrode when welding current is flowing. The weld puddle directly behind the arc is re-exposed to the surrounding water immediately after arc passage. Consequently, unlike welds made in air, wet SMA welds are subjected to rapid cooling known as quenching. Quenching is the primary cause of poor quality in wet SMA welds.

Quenching causes the formation of martensite in the heat affected zone (HAZ) of the weld. The HAZ is the section of the weld that has been heated to above the A1 transformation temperature (723 degrees C) but has not reached the melting point. If the rate of cooling from the transformation temperature to ambient temperature is sufficiently rapid, a needle-like structure called martensite will be formed. The crystal structure of un-tempered martensite inhibits dislocation movement. Consequently, this form of martensite is non-ductile. Untempered martensitic HAZs cause welds to be brittle, hard, and to lack toughness.

Arc electrolysis produces atomic hydrogen and oxygen which diffuse into the weld pool. Quenching traps these gases in the weld because the outward diffusion rate through the rapidly solidifying metal is much slower than initial diffusion into the molten weld pool. Entrapped hydrogen reduces weld ductility through the "cold cracking" mechanism. Over time, hydrogen atoms in the weld migrate to interstitial voids where they recombine to form hydrogen gas. Pockets of hydrogen gas produce tensile stresses that can initiate trans-granular cracks. (This phenomena has been termed cold cracking because it generally occurs after the weld has cooled to approximately 200 degrees C). Oxygen in the weld produces pores which reduce strength and toughness.

Quenching also traps non-gaseous contaminants such as oxide slags in the weld metal. These contaminants are generally less dense than iron and would float to the surface of the weld pool under gradual cooling conditions. Their entrapment further increases weld porosity.

In addition to micro-structural and chemical effects, quenching produces steep thermal gradients with resultant high residual stresses, thereby increasing weld susceptibility to crack initiation upon exposure to environmental loading. Finally, quenching has been shown to increase weld bead convexity (reinforcement) leaving welds more susceptible to toe cracking [2].

In summary, wet SMA welds are inherently brittle, porous, and susceptible to cracking, and all of these traits can be attributed directly or indirectly to rapid weld cooling.

2.2 Material Limitations of Wet SMA Welding

Because of weld quenching, wet SMAW cannot be used to join certain materials. Most important among these are steels that derive their material properties from thermal treatment (such as quenching and tempering). Low alloy (less than 0.2% carbon), high yield strength, quenched and tempered steels (HY steels) are used widely in the construction of naval surface combatants and submarines. Yield strengths of up to 130 ksi are achieved in these steels by quenching low-carbon alloy steel so that a desired amount of martensite is formed. Because of impedance to dislocation flow, martensite is strong but it has poor toughness. After quenching, the alloy is heated to a maximum temperature below A1, and gradually cooled to ambient temperature. This procedure is known as tempering; it causes the martensite to be softened so that toughness is increased, and if properly performed can result in only a minor loss of strength. (The tempering temperature and cooling profile are dependent on the desired mechanical properties of the steel being produced). The HAZ of an SMA weld made in a high yield strength quenched

and tempered steel will in general have been heated to above the tempering temperature and then cooled more rapidly than the tempering profile. This is especially true in the case of wet welds. Consequently, the tempered martensitic structure will have been transformed into brittle martensite. The result is a non-ductile HAZ that is susceptible to cracking. In an experiment performed jointly by Batelle Industries and MIT, it was found that all cracking in experimental HY-80 weldments originated in the HAZ [3]. Cracking susceptibility is further increased in wet welds because of the relatively large amounts of hydrogen that they absorb.

In surface welding and dry underwater welding, base plates can be preheated and post-heated using electrical resistance. These procedures offset HAZ cooling and reduce or eliminate the loss of toughness in HY steels. Electrical resistance heating of submerged base plates is not feasible. Hence, because of rapid cooling rates, inability to supply active heating, and hydrogen absorption, wet SMAW cannot be used to weld quenched and tempered HY steels.

In addition to HY quenched and tempered steels, martensite is formed in the HAZs of weldments with relatively high carbon content. Carbon contents of steels are often compared using an index known as carbon equivalent (CE). (Actually CE is a measure of both carbon content and, to a lesser extent, the contents of various other alloying elements. Positive coefficients are assigned to alloying elements that generally inhibit weldability, and negative coefficients to elements that improve weldability). Different definitions of CE are encountered in the literature. The most common definition is presented below in equation {2.1}.

$$\%C + \frac{\%Mn}{6} + \frac{\%Cr}{10} - \frac{\%Mo}{50} - \frac{\%V}{10} + \frac{\%Cu}{40} + \frac{\%Ni}{20} \quad \{2.1\}$$

The American Welding Society (AWS) has defined a specific relationship to be used when computing CEs for wet SMAW. This definition—equation {2.2}—is more conservative (i.e., gives a higher CE for an equivalent material) than equation {2.1} in recognition of the technical difficulties associated with wet SMAW.

$$\%C + \frac{\%Mn}{6} + \frac{\%Cr + \%Mo + \%V}{5} + \frac{\%Ni + \%Cu}{15} \quad \{2.2\}$$

Masubuchi et. al. demonstrated a direct relationship between carbon content and martensitic hardening in the HAZs of various steels [4]. Because of this relationship the U.S. Navy has restricted the use of wet SMAW to base plates with CEs of less than 4.0.

2.3 Technological Advances in Wet SMAW

During World War II, U.S. Navy divers coated standard SMAW electrodes with paint to protect the flux so that the electrodes could be used underwater. Since then, improvements in wet SMAW technology have included (1) better electrode waterproofing materials and procedures, (2) specifically designed fluxes for underwater use, and (3) most recently, the introduction of specialized electrodes for underwater SMAW. In all cases, the primary goal has been to reduce the amount of hydrogen admitted into the weld.

Reducing the amount of water absorbed by electrode fluxes is a basic technique for limiting hydrogen input to a weld. Water in flux decomposes to hydrogen and oxygen when subjected to arc energy densities. These diatomic gases and their respective ions can then be absorbed into the molten weld pool. Furthermore, water trapped in flux can vaporize when an arc is struck and explode the flux off of the electrode leaving it unprotected. Waterproofing of electrodes for underwater use has evolved from painting to a regimented procedure of electrode baking to remove absorbed water from the flux, followed by coating with low-permeability epoxies or thermoplastic lacquers. Water intrusion tests have demonstrated that properly prepared electrodes will gain less than 0.02% of their original weight when exposed to water for a period of six hours [5].

Specialized chemical compositions have been formulated for wet welding fluxes. These proprietary fluxes burn significantly more slowly than the core wire melting rate, thereby providing a protective cavity for the arc and preventing side arcing in the contact drag technique often used in wet SMAW. They have low hydrogen content and are designed to be highly exothermic. Reduced hydrogen content limits direct hydrogen input to the weld from the flux. Hot burning fluxes increase arc temperature so that more heat is imparted to the base metal thereby partially offsetting quenching and promoting weld off-gassing. Wet welding fluxes also contain oxidizing agents that bond with hydrogen and iron in the base metal forming iron hydroxides, consequently further limiting hydrogen input to the weld.

Results of two studies have shown that the types of currently available wet welding electrode fluxes that are the most successful in reducing hydrogen input to a weld are rutile (TiO_2) and iron powder/oxidizing iron oxide fluxes [6,7].

A.W. Stalker measured residual H_2 content in deposited weld metal at 650 deg. C and found it to be significantly lower (by as much as 92%) for rutile and iron powder fluxed electrodes than for any other type of flux studied [8]. (It should be noted that in the majority of the literature, flux and core wire parameters are not investigated separately. Thus, one cannot be certain that reported results can be solely attributed to flux

14

composition changes, since the results may have been influenced by differences in core wires.)

Coincident with flux development, progress has been made in determining the suitability of specific core wire types for wet welding. In two separate wet SMAW electrode evaluations, ferritic electrodes produced the highest quality welds. (Ferritic steel is composed of body center cubic "alpha" iron with minor additions of carbon and other alloying elements.)

In 1990, Welding Engineering Services Inc. and the Naval Sea Systems Command conducted an evaluation of eight electrodes specifically designed for wet SMAW at Norfolk Naval Shipyard. Fillet and butt weids were made in steel plates with carbon equivalents ranging from 0.350 to 0.449. Welds were made in a tank and in the Elizabeth River. Destructive and non-destructive testing of the completed welds resulted in an E7014 ferritic electrode being given the highest weldability rating. Welders were able to produce sound welds in base plate with CEs of 0.406 and below using this electrode. Of the other electrodes tested, austenitic core wires had the poorest weldability, producing underbead cracks over the full range of CEs evaluated [6]. (Austenite is face center cubic "gamma" iron that has been stabilized to room temperature by addition of alloying elements such as nickel and chromium.)

A Welding Institute evaluation also concluded that ferritic electrodes—specifically those coated with an iron-oxide flux—produced the best wet SMA welds. The evaluators postulated that the success of the ferritic electrodes was a result of their relatively pure iron deposits (only small amounts of alloying elements). The resultant welds had low yield strengths that reduced stresses during loading thereby inhibiting crack formation [8]. In essence, the ferritic electrodes were "undermatched" and the welds were able to yield plastically, and thus retard crack initiation. The investigators in this study also had some success with "fully" austenitic electrodes. They concluded that good welds were obtained with austenitic electrodes because of the relatively high hydrogen solubility of gamma iron.

The differences in the results of the two evaluations may be attributed to a lower percentage of gamma iron in the austenitic electrodes used in the Naval Sea Systems Command study.

Improvements in wet SMAW electrodes, electrode fluxes, and waterproof coatings have made it possible to produce satisfactory welds in limited situations, such as low carbon non-heat treated steel joints that will not be subjected to high levels of

environmental loading. Further improvements in wet SMA weld quality, and a broadening of the range of materials that could be joined using wet SMAW, could be realized through solution of the primary problem associated with this process: rapid weld cooling.

CHAPTER 3. REDUCTION OF WELD COOLING RATES
THROUGH THERMAL INSULATION

Bouaman and Haverhals demonstrated that the cooling rates of wet SMA welds are inversely related to the thickness of the plate being welded, up to a limiting thickness. At thicknesses above the limiting value, cooling rates increase with plate thickness until a second limit is reached above which cooling rates are approximately unaltered by further thickness increases [9]. The authors contrasted this result with the direct relationship between cooling rate and plate thickness in dry SMA welds. Welds made in air demonstrate this direct relationship up to a limiting thickness value above which cooling rates (the inverse of cooling times) are not a function of plate thickness (see figure 3.1).
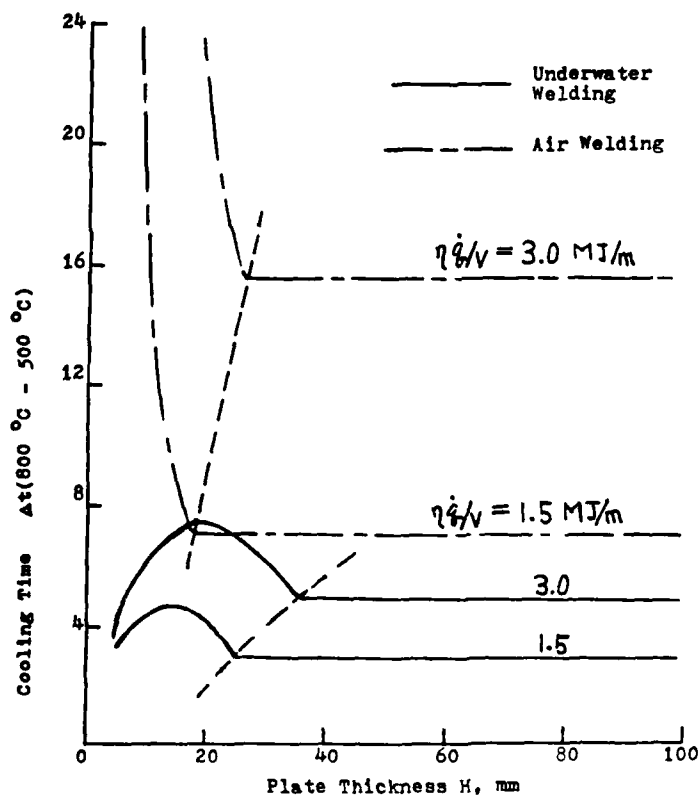
Figure 3.1 Cooling Time vs. Plate Thickness in Wet and Dry Welds
for Two Heat Input Values [9]

The thickness limit value for dry welds can be assumed to be the semi-infinite-body dimension for the heat input and boundary heat losses associated with the welding parameters being evaluated. A rough estimation of the validity of the semi-infinite-body assumption can be made by using a solution to the non-dimensionalized unsteady heat diffusion equation. (The unsteady heat diffusion equation will be discussed in detail in the following chapter.) If $\delta_{(0.99)}$ is defined as the minimum perpendicular distance— from a heat source through a given material—at which temperature is not affected by the source, then it can be shown that:

$$\delta_{(0.99)} = 3.65\sqrt{\alpha t} \qquad \{3.1\}$$

Alpha is the thermal diffusivity of the material and t is the characteristic exposure time for the heat source. For steel, α is on the order of 4×10^{-6} m^2/s. The characteristic exposure time is the time required for the weld puddle to move past a given point on the surface of the plate. A value of 3 seconds is reasonable for this parameter assuming approximately 9 inches per minute arc travel speed. Substitution of these values into equation 3.1 yields $\delta_{(0.99)} = 13$ mm. This value is reasonably close to the limiting thicknesses for dry welds shown in figure 3.1.

The wet welding relationship is more complicated. It is possible that in progressing from very thin to moderately thicker plates, peak temperature will increase as the thermal diffusivity of the submerged plate system decreases (because of increased thermal resistance). Plates thinner than the first limit thickness have almost no conductive resistance so that heat input to the plate is rapidly convected back to the water from both the top (side being welded) and bottom of the plate. Conductive resistance increases and convection from the back of the plate decreases as thickness is increased toward the first limit, consequently cooling rate slows. The first limiting thickness would then represent attainment of equilibrium between the available arc heat flux into the plate and the boundary heat losses. Maximum peak temperature would be reached at this limit and peak temperature would then remain unchanged with further increases in plate thickness. Cooling rates rise with increases of thickness above the first limit because of the greater conductive capacity of the plate. As thickness is increased beyond the first limit, back side convection is further decreased; however, the greater conductive capacity of the plate allows heat to be transferred in the plane perpendicular to the through-thickness direction and back to the top surface of the plate, away from the weld. The second limit would then represent the semi-infinite-body dimension for the wet weld.

An attempt was made to test this hypothesis by examining the non-dimensional Biot Number (Bi), which represents the ratio of conductive and convective thermal resistances for a given heat transfer problem.

$$Bi = \frac{hL}{k} \qquad \{3.2\}$$

where:
       h=convective heat transfer coefficient (W/m^2K)
       L=characteristic length (m)
       k=conductivity (W/mK)

For wet welding of mild steel, Tsai proposed an average surface heat transfer coefficient of approximately 1200 W/m^2K [2]. The conductivity of mild steel is on the order of 35 W/mK. In this analysis, the characteristic dimension is plate thickness. When the first limit value for wet welds (as determined by Bouaman and Haverhals) of $\cong$ 0.02m (0.75 inches) and the aforementioned heat transfer and conductivity values are used to compute Bi, a result of approximately unity is obtained. The relative magnitudes of conductive and convective heat losses are similar. Consequently, a decision with respect to the validity of the hypothesis being tested cannot be made on the basis of this rough analysis. However, the analysis does demonstrate that convective heat transfer is at least as important as conductive cooling in wet welds. (This is not the case for dry welds which, because of the lower convective cooling capacity of air, have Biot numbers on the order of 0.1. Conductive cooling dominates dry SMA welds.) Of further importance is the fact that Tsai's estimate of the average convective heat transfer coefficient in wet welds may be quite conservative. Tsai assumed that nucleate boiling did not take place on the surface of the plate being welded. Nucleate boiling on the plate surface could increase the effective convection heat transfer coefficient by several orders of magnitude.

The results of these analyses indicate a potential practical application of thermal insulation of wet welds. Specifically, thermal insulation could be used to significantly reduce wet weld quenching by slowing the rate of convective heat loss to the surrounding water.

3.1 Experimentation with Insulation of Wet Welds

MIT conducted a series of underwater welding experiments from 1974 to 1976 [10]. The experiments were conducted in the MIT welding laboratory and in the Baltic

19

Sea. Two of these studies investigated methods of thermally insulating wet metal arc welds.

In the first study, MIT investigators developed flux shielded welding in an attempt to reduce wet weld quenching. In this process, a continuous blanket of molten flux is used to shield the arc area from surrounding water. A consumable electrode is fed through the flux and into the weld zone. An arc is initiated when the electrode contacts the base plate. The process is similar to submerged arc welding. Two methods were initially developed to create the flux blanket. In the flux-feed method, liquid flux is continuously supplied to the weld area. This method proved technically difficult because of flux freezing problems and was abandoned. In the flux-stuffed-enclosure method, welding flux is placed in an enclosure that is pre-aligned with the joint. This is the method that was tested in the Baltic Sea. After welding, measurements of weld metal and HAZ hardness were made.

Steel hardness values can be correlated to micro-structure which can in turn be used to estimate cooling rates. For a particular grade of steel, post-weld hardness increases with martensite content. With a known martensite content, the cooling rate can be estimated with the Continuous Cooling Transformation (CCT) diagram for the steel being welded. An example of a CCT diagram with superimposed cooling curves is presented in figure 3.2.
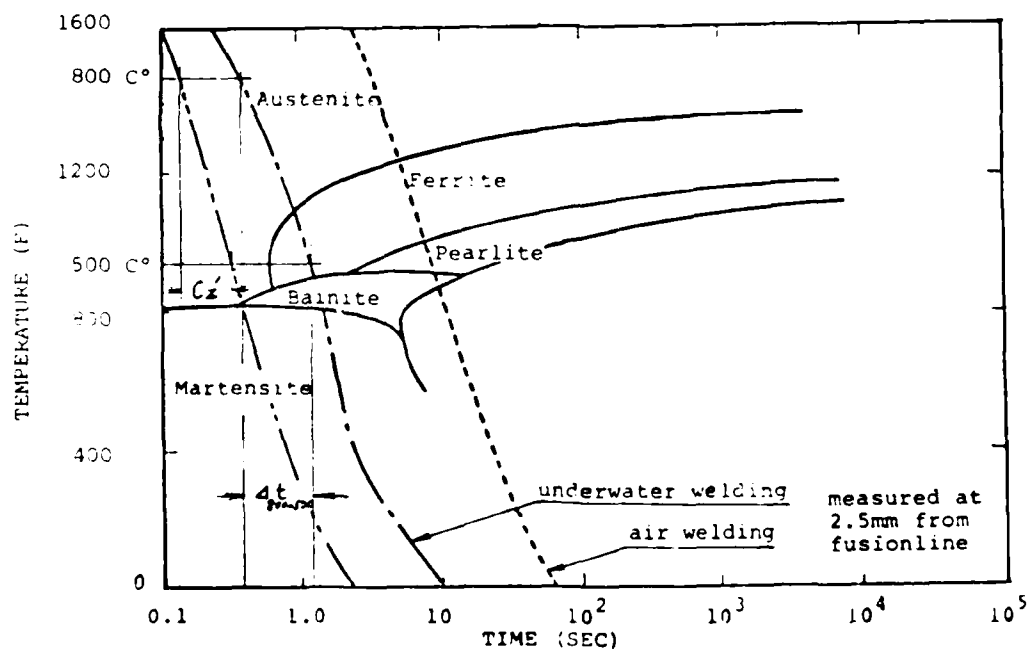
Figure 3.2 Weld Cooling Curves Superimposed on a CCT Diagram [10]

20

Hardness testing results from the flux shielded welds were inconclusive. They exhibited lower weld metal hardness values than unprotected wet SMA welds by 10 to 30%. However, HAZ hardness in the flux shielded welds was 6 to 30% higher than in the unprotected welds. Reasons for this inconsistency were not determined.

More important than the experimental results were the technical difficulties encountered with flux shielded welding. Flux enclosure to joint alignment was difficult, so test welds were made only on the simplest joint geometries. Some experimental results were identical to those obtained with unprotected wet SMAW. The investigators postulated that in these cases incomplete shielding was attained and water intruded into the weld area. In addition to the difficulties noted by the investigators, another problem associated with practical application of flux shielded welding is joint orientation. Many underwater welds are performed in the overhead and vertical positions. Keeping flux against a joint in these positions would be extremely difficult. It is conceivable that these problems could be solved and that satisfactory flux shielded welds could be made in all positions. However, it is unlikely that the resulting process would be more flexible or less expensive than dry underwater welding. The experimental results showed that welds made with the flux shielding process were inferior to welds made in air (the former had both harder weld metal deposits and HAZs). A process that produces more inferior welds than dry welding but does not increase flexibility or reduce cost is not viable.

In addition to the aforementioned technical problems, there is a significant operational barrier to the flux shielded welding process: the welder cannot see the joint. Welding, which is both a visual and tactile process requires hand-eye coordination. Elimination of visual feedback is a severely negative aspect of any manual welding process. Automated processes may depend less on visual feedback than manual ones, but few underwater welding applications are currently automated. Processes that block welders from seeing their work have generally not been applied commercially.

In 1982 Satoh, et al. developed a method of retarding cooling in wet welds mainly by attaching a thermal insulation shield to a GMAW torch [11]. The shield was used in conjunction with insulation strips of moderate thermal resistance that were placed adjacent to the weld. The primary shield extended from the torch parallel to the weld line so as to shield the weld from water both immediately before and after arc passage. The shield also extended perpendicular to the weld line, contacting the side insulation strips (see figure 3.3 on the following page).
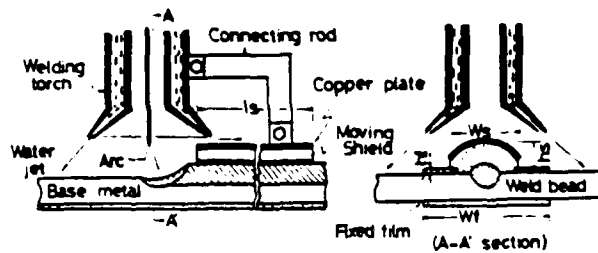
Figure 3.3 Schematic of the Local Drying Method Developed by Satoh [11]

Satoh's local drying method proved moderately successful in reducing wet weld cooling rates. However, it was not patented and no commercial application of this process has been encountered by this author. It is likely that torch shield blockage of the welder's arc view is the reason that this process has not been commercially accepted.

The second experiment that was conducted during the 1974-76 MIT underwater welding study was an investigation of the effects of static insulation on wet SMA weld cooling rates. One-eighth-inch-thick asbestos cloth insulation strips were placed on 0.75-inch-thick mild steel plate, and bead-on-plate wet SMA welds were made. Varying insulation geometries were tested. The size of the weld HAZ was used as an estimate of temperature penetration for this experiment. Insulating the side of the plate being welded—with the exception of a narrow strip centered on the weld line—had the greatest effect on HAZ size, causing it to increase by as much as 28%. Full insulation of the plate back side also enhanced thermal penetration. In these cases, up to 20% increases in HAZ size were achieved.

It is possible that increased peak temperatures caused by greater thermal diffusion into the base plate—as a result of decreased convective cooling—could reduce weld cooling rates. More heat must diffuse away from the weld. This diffusion is slowed due to the increased thermal resistance of the system imposed by the insulation strips. The MIT investigators postulated that insulation could reduce nucleate boiling on the surface of the plate and interfere with film boiling on the back side. Nucleate boiling convective heat transfer coefficients are approximately two orders of magnitude greater than those for film boiling. The investigators therefore concluded that the most effective location for static insulation was the front surface of the plate being welded.

Support for the aforementioned hypothesis can be found in an article published in 1971 by Bouwman and Haverhals, who achieved a 20% reduction in the 800 - 500 deg. C cooling rate of a wet SMA weld by using an insulation layer of unspecified material on the surface of the plate being welded [9].

22

3.2 Practical Use of Insulation

A potential practical method for reducing cooling rates in wet SMA welds—that has not been rigorously examined—is the use of high thermal resistance insulation on the surface of the plate being welded. The previously discussed experimental results demonstrate that the front surface of a plate that is being welded is the most effective location for insulation. Fortunately, this is also the most practical location. The surface of any structure that is to be welded must be accessible. In general, this is not true of the back side, particularly in underwater welding. The back side of floating or sunken ship compartments or appendages is rarely accessible. The internal sections of tubular structural members used in offshore oil platform construction are normally flooded or grouted and cannot be accessed. Placement of flow-restricting insulation on the inside of pipelines is impractical. Thus, the optimum location for insulation from both thermal and operational considerations is the welding surface.

Insulation strips could be placed adjacent to the joint on the surface of the structure being welded and would therefore not block the welder's view of the arc and weld puddle. If it is determined that the insulation must directly abut the joint line, then the strips could actually facilitate welding by serving as electrode guides.

Computational modeling can be used to quantify the effects of aggressive surface insulation on wet weld cooling rates and to determine the material requirements of potential insulation materials.

CHAPTER 4. COMPUTATIONAL THERMAL MODELING
OF A WET SMA WELD

In the previous chapter it was shown that convection is an important boundary heat-loss mechanism in wet SMA welds. Surface insulation of the material being welded could potentially reduce convective heat losses, thereby increasing peak temperature and reducing cooling rate in the HAZ. This chapter describes a computational model of a wet SMA weld that was used to quantify the potential effects of surface insulation, to determine optimum insulation geometries, and to estimate the required thermal stability of potential insulation materials.

4.1 History of Wet Weld Analytical and Computational Models

Tsai's parametric study of wet weld cooling phenomena [2] was the most extensive source of information on analytical and computational modeling of wet welds encountered in the literature. The author presented a detailed history of analytical attempts at modeling wet welds. He found that in all cases the analytical models predicted cooling rates and peak temperatures that significantly exceeded experimental values. Tsai concluded that the wet welding process was too complicated to be successfully modeled analytically. Multiple factors—bubble dynamics and liquid flow fields around the weld; arc thermal losses to the environment; and phase changes in the electrode, flux, base metal and surrounding water—combine with a geometrically complex weld pool; conduction, and natural and boiling convection heat losses; and a moving heat source to create a multi-variable highly nonlinear problem. He proposed a combined numerical/semi-empirical approach for modeling wet welds.

Tsai conducted a numerical finite-difference analysis of wet SMA welds using empirically determined boundary heat-loss relationships. His computed predictions were closer to experimental results than previous analytical work but still predicted faster cooling rates and higher peak temperatures than the experimentally determined values.

4.2 General Modeling Method

The purpose of this research is to determine the effects of thermal insulation on wet SMA welds. Computational modeling is used only to estimate these effects. Consequently, a detailed model—refined continuously in an attempt to exactly duplicate experimental results—is not necessary. (Because of the relatively small number of wet weld thermal measurements that have been made, there is not a large data base from which to statistically estimate the accuracy of any given experiment. Therefore, attempts

to exactly reproduce experimental results with computational procedures are not warranted). For this study, simplifying assumptions were made wherever justifiable, and pre-tested, commercially available computational methods were used.

The commercial spectral element program Nekton™, available through Nektonics Incorporated, was used to perform the computational analysis. Nekton is capable of performing heat transfer and fluid flow computations. It is classified as a spectral element program because it is capable of defining element boundaries by high order (i.e., n=7) polynomials. This is particularly useful for fluid flow and melting front analyses. With the primary exception of element boundary definition, Nekton functions similarly to other available finite element (FE) programs. The Nekton source code is FORTRAN 77.

The following paragraphs describe the mathematical procedure used to model the unsteady heat conduction problem presented by a wet SMA weld. The governing equation and boundary conditions are cited. The solution method is generalized due to the proprietary nature of the Nekton source code.

Equation {4.1} is the specific form of the Energy Equation used to analyze heat transfer. It is the generalized, three-dimensional (3-D), unsteady heat conduction equation.

$$\frac{\partial}{\partial X}(kx\frac{\partial T}{\partial X}) + \frac{\partial}{\partial Y}(ky\frac{\partial T}{\partial Y}) + \frac{\partial}{\partial Z}(kz\frac{\partial T}{\partial Z}) + Q - \rho Cp\frac{\partial T}{\partial t} = 0 \qquad \{4.1\}$$

where:
Q = volumetric heat generation
kx, ky, kz = directional heat conduction coefficients
ρ = density of conducting material
Cp = constant pressure heat capacity

The relevant flux and convection boundary conditions are represented in equation {4.2}.

$$kx\frac{\partial T}{\partial X}lx + ky\frac{\partial T}{\partial Y}ly + kz\frac{\partial T}{\partial Z}lz + q + \alpha(T) = 0 \qquad \{4.2\}$$

where:
q = specified boundary heat flux
$\alpha(T)$ = specified boundary convective heat loss
lx, ly, lz = direction cosines of the outward normal to the boundary surface

If the material is isotropic—such that kx = ky = kz ≡ k—and boundary flux and convection are set equal to zero, {4.2} simplifies to {4.3}, the insulation (0 flux) boundary condition.

25

$$\frac{\partial T}{\partial n} = 0 \qquad \{4.3\}$$

where:
        n = vector normal to boundary surface

In the case of wet SMA welding, volumetric heat generation is zero, and the steel being welded is isotropic. Consequently, {4.1} and {4.2} simplify to {4.4} and {4.5} respectively.

$$k(\frac{\partial^2 T}{\partial X^2} + \frac{\partial^2 T}{\partial Y^2} + \frac{\partial^2 T}{\partial Z^2}) - \rho C p \frac{\partial T}{\partial t} = 0 \qquad \{4.4\}$$

$$k(\frac{\partial T}{\partial X} lx + \frac{\partial T}{\partial Y} ly + \frac{\partial T}{\partial Z} lz) + q + \alpha(T) = 0 \qquad \{4.5\}$$

Equations {4.4} and {4.5} were solved simultaneously using Nekton. The first step in finite element iterative solution of partial differential equations such as {4.4} and {4.5} is formation of the content function in accordance with Euler's Theorem. The combined content function for equations {4.4} and {4.5} is given by equation {4.6}.

$$\Phi = \iiint [\frac{k}{2}[(\frac{\partial T}{\partial X})^2 + (\frac{\partial T}{\partial Y})^2 + (\frac{\partial T}{\partial Z})^2] + (\rho C_p \frac{\partial T}{\partial t})]dxdydz +$$

$$\iint qT ds + \iint_2 (\frac{\alpha}{2})T^2 ds \qquad \{4.6\}$$

where:
      Φ = content function
      c1 = area of prescribed flux boundary condition
      c2 = area of prescribed convective boundary condition

The derivative of the content function is then formed for each element with respect to a specific nodal temperature. Results of this operation are shown in equation {4.7}. (In this 3-D example, a tetrahedral element with nodes i, j, k, and l is assumed for notational simplicity. In the actual model, parallel-piped elements were used).

$$\frac{\partial \Phi'}{\partial T} = \iiint [k[\frac{\partial T}{\partial X} \frac{\partial}{\partial T_i}(\frac{\partial T}{\partial X}) + \frac{\partial T}{\partial Y} \frac{\partial}{\partial T_i}(\frac{\partial T}{\partial Y}) + \frac{\partial T}{\partial Z} \frac{\partial}{\partial T_i}(\frac{\partial T}{\partial Z})] +$$

$$\rho C_p (\frac{\partial T}{\partial t}) \frac{\partial T}{\partial T_i}]dxdydz + \iint q \frac{\partial T}{\partial T_i}ds + \iint_2 \alpha T \frac{\partial T}{\partial T_i}ds \qquad \{4.7\}$$

Temperature (T) is a function of position within a specific element.

$$T = [N_i, N_j, N_k, N_l][T]^e \qquad (4.8)$$

where:

N_i through N_l are position functions

$[T]^e$ is the nodal temperature vector

A sample position function for a tetrahedral element is given in equation (4.9) [12], and equation (4.10) defines the nodal temperature vector.

$$N_i = \frac{(a_i + b_i X + c_i Y + d_i Z)}{6V} \qquad (4.9)$$

where:

a_i, b_i, c_i, d_i = position constants specific to the FE program
($b_i = c_i = d_i$ for isotropic materials)
V = volume of the tetrahedral element

$$[T]^e = \begin{bmatrix} T_i \\ T_j \\ T_k \\ T_l \end{bmatrix} \qquad (4.10)$$

Equations (4.8) and (4.9) are substituted into equation (4.7), which is then summed over all nodes. The result (equation (4.11)) is an expression for the temperature derivative of the content function of an element that is dependent on $[T]^e$, position constants, element size, and—if the element has an external face—prescribed values of flux and convective heat loss.

$$\left[\frac{\partial \Phi}{\partial T}\right]^e = \begin{bmatrix} \dfrac{\partial \Phi^e}{\partial T_i} \\[6pt] \dfrac{\partial \Phi^e}{\partial T_j} \\[6pt] \dfrac{\partial \Phi^e}{\partial T_k} \\[6pt] \dfrac{\partial \Phi^e}{\partial T_l} \end{bmatrix} = [h][T]^e + [p]\left[\frac{\partial T}{\partial t}\right]^e + [f] \qquad (4.11)$$

27

Matrix [h] is an analog of the stiffness matrix used in structural analyses. The last two terms in equation (4.11) arise from the unsteady nature of the problem. Finally, equation (4.11) is summed over all elements and extremized, as shown in equation (4.12)

$$[H][T] + [P]\left[\frac{\partial T}{\partial t}\right] + [F] = 0 \qquad (4.12)$$

The problem is fully posed upon substitution of initial temperature values into (4.12). This compound matrix equation can then be solved by a number of iterative techniques such as Gaussian elimination or LR-LU decomposition.

4.3 Modeling Procedure

The Nekton pre-processing subroutine was used to build a three-dimensional model of a mild steel plate surrounded by water. The model was scaled so as to duplicate the mild steel plate used by Tsai in his experimental measurement of cooling rates in uninsulated wet SMA welds [2]. This procedure was followed so that computed results could be compared with Tsai's experiments to provide a feel for the validity of the model. Insulation effects were then studied—after the baseline (uninsulated) model had been validated—by specifying insulation boundary conditions at desired locations on the baseline model.

In constructing the baseline model, symmetry was invoked to reduce the volume of the plate that had to be modeled. A zero flux boundary condition was imposed on the Y-face of the plate directly below the welding arc, which was at the centerline of the plate in the Y direction. The change in temperature with respect to Y is zero on this face due to symmetry. Therefore, only half of the plate had to be modeled. A simplified schematic of the baseline model is shown in figure 4.1 on the following page. (Element mesh density in figure 4.1 is substantially less than that used in actual computations so that prominent features can be plainly depicted).

Conductivity, density, and heat capacity values for mild steel (0.15% carbon) were assigned to the modeled plate. These values are listed in table 4.1.

Table 4.1 Material Parameters of the Mild Steel Plate Model

k (W/mK)	ρ (Kg/m^3)	Cp (J/KgK)
35.91	7833	465
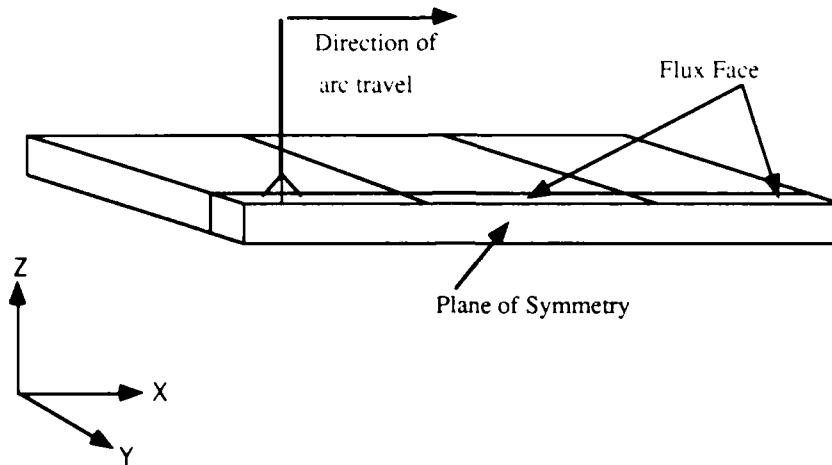
Figure 4.1 Baseline Model Schematic

An input file was written specifying flux and convection boundary condition locations. Zero flux was specified at the symmetry plane. Tsai's empirically determined convective heat transfer coefficient (HC) relationship was used to define convective boundary losses over all surfaces of the plate with the exceptions of the symmetry plane and the flux strip. This relationship and the associated convective heat flux (q_c) are defined in equations {4.13} and {4.14} respectively.

$$HC = 3309.2(TEMP - TINF)^{\frac{1}{4}} \ [\text{W/m}^2\text{K}] \qquad \{4.13\}$$

where:
TEMP = plate surface temperature
TINF = initial temperature of water and plate

$$q_c = 3309.2(TEMP - TINF)^{\frac{5}{4}} \ [\text{W/m}^2] \qquad \{4.14\}$$

To simulate a traveling arc, a time-dependent flux boundary condition was established over the Z-face of the flux strip elements. Values for arc power, arc efficiency, and travel rate—corresponding to the respective values from Tsai's experiment—were used. Arc flux (q) was calculated as shown in equation {4.15}.

29

$$q = \frac{A_v A_i}{2\pi(A_r)^2}(\eta_a) \qquad \{4.15\}$$

where:

A_v = arc voltage

A_i = arc current

A_r = arc radius (approximately equal to electrode radius)

η_a = arc efficiency

The factor of two in the denominator of equation {4.15} is required because the model has been cut in half at the symmetry plane. Arc efficiency is difficult to measure for wet welds. Tsai used a semi-empirical analysis to estimate a wide range of arc efficiencies (0.36-0.70) for wet SMA welds. The mean value of this range—0.53—was input to equation {4.15}. The flux strip was divided into elements with Z-face areas approximately equal to arc area. A sequential time step (dt) was established and set equal to the amount of time a point on the plate surface would be exposed to the arc, given the specified travel speed and arc size. For this model, dt=1.25 seconds. Movement of the arc was initiated at X=0, and time (t)=0. The calculated flux q was imposed over the Z-face of the first element in the flux strip (starting from X=0) for time dt. At t=dt, flux over the first element is set equal to zero, flux over the Z-face of the next flux strip element in sequence is set equal to q, and time is incremented, t=t+dt. This procedure was repeated until the simulated arc had traveled the full length of the flux strip.

To record HAZ surface cooling, a history point was established on the surface of the plate (Z=0), at the X-axis midpoint, and 0.5 cm off of weld centerline (Y=0.005 m). The Y position corresponded to the location of a thermocouple used in Tsai's experiment to measure HAZ surface cooling. The centerline X-position was chosen to minimize edge effects. History point temperature at the end of each time step was recorded and stored in a history file. After removal of arc flux from the final element, time incrementation was continued until thermal equilibrium had been reached at the history point.

The FORTRAN computer code used to specify thermal parameters, construct a model geometrically, create elemental mesh, and position history points for a typical model is presented in appendix A. Appendix B is the computer code used to establish boundary conditions, including simulated arc travel.

4.4 Verification of the computational model

Figure 4.2 compares computed and experimental HAZ cooling rates.
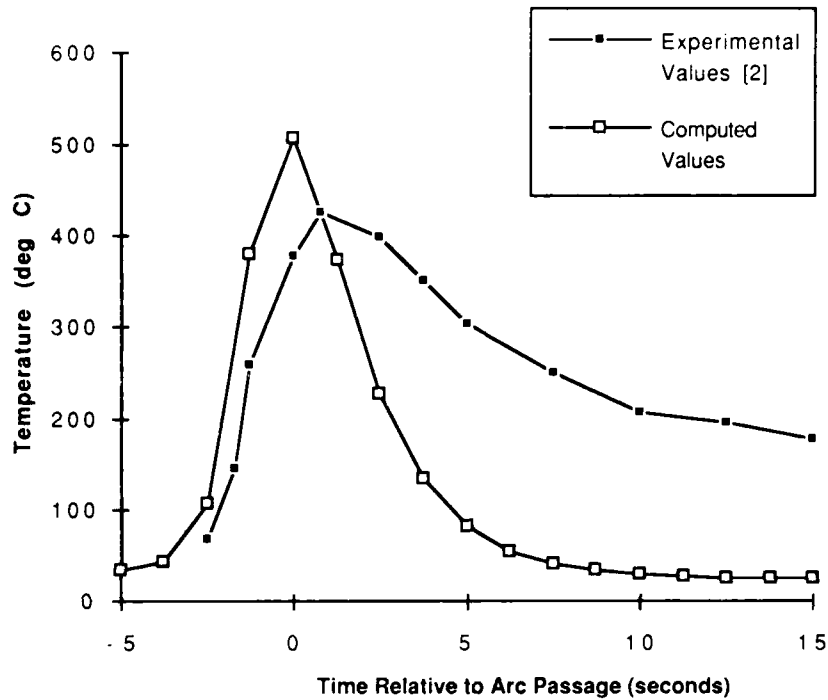
- Arc Power = 5000W and arc efficiency = 0.53
- Travel speed = 22.86 cm per minute (9 inches per minute)
- Electrode wire diameter is 0.47625 cm (3/16 inches)
- Ambient temperature = 24.4 degrees C
- Experimental values taken from C.L. Tsai [2]

Figure 4.2 Temperature on 0.635 cm (0.25 inch) thick mild steel plate surface at a distance of 0.5 cm from weld centerline

Computed peak temperature is slightly higher than the experimental value. More significantly, the model predicts a faster cooling rate than that measured experimentally by Tsai. By reducing both the arc efficiency and the heat transfer coefficient constant, the computed results can be made to closely match experimental values. Based on the arc

efficiency range postulated by Tsai, reducing the modeled arc efficiency to any value between 0.36 and 0.53 would be reasonable. Additionally, Tsai's empirically derived expression for HC is based on a log-log linear plot of 17 data points. Adjustment of the slope of this line (i.e., the constant in equation [4.13]) could be justified. However, such adjustments would serve no scientific purpose. The values of both parameters are not well established, and both would have to be altered to force the computational model into agreement with experimental results (peak temperature and cooling rate are functions of both arc efficiency and the convective heat transfer coefficient). Thus, no increase in the certainty of either parameter value would be obtained, because alignment with experimental results could not be attributed to a change in one specific parameter. Additionally, since Tsai's work was the only wet weld cooling rate data encountered, manipulation of model parameters would be an attempt to exactly match the results of a single experiment and would thus not be warranted.

Figure 4.3 on page 33 demonstrates a further validation of the computational model. Cooling rate in a one-inch-thick plate is computed to be initially faster than in a quarter-inch-thick plate. This is in agreement with the experimental data presented in figure 3.1.

Computed values correspond reasonably well with experimental results. Therefore the model can be used to *estimate* the effects of thermal insulation on wet weld cooling rates. However, it is important to note that the model is a simplified simulation of a complex process. Significant assumptions will be discussed briefly in the following paragraphs.

Weld bead heat loss to the environment after arc passage has been set equal to zero for all computations. This is a justifiable assumption based on Tsai's analytical estimate of negligible heat loss from a completed weld bead. The assumption can be justified on a physical basis because SMA weld beads are covered with metal oxide slags—formed by flux decomposition—as they are being deposited. Metal oxides (ceramics) are excellent high temperature insulators.

The base metal heat conduction parameter (k) has been assumed to be constant throughout the plate. In reality, k is a weak function of temperature for a given phase, and can change dramatically with phase changes in a material. Thus, the conduction parameter for molten steel (k_l) is less than that for solid steel (k_s) (although the effective value of the former may actually be greater due to convection currents). The volume of base metal that melts in a SMA weld is small in comparison to the volume of the plate, and the melt zone boundaries are difficult to define mathematically. These factors combined with the wide range of $(k_s)/(k_l)$ ratios for steel encountered in the literature

(these values ranged from 1 to 2) led to the simplifying assumption of constant k throughout the plate.
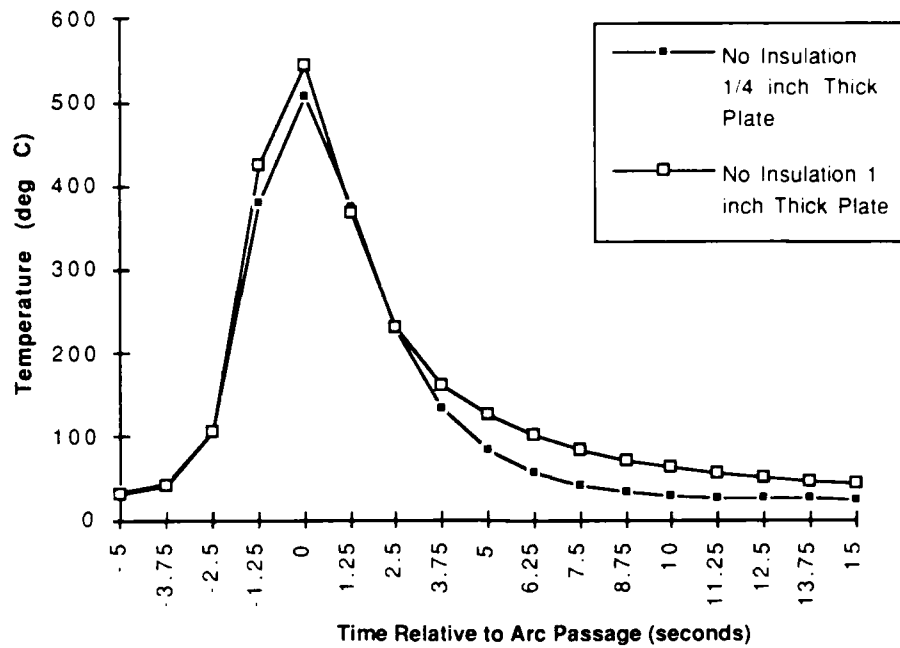
- Arc Power = 5000W and arc efficiency = 0.53
- Travel speed = 22.86 cm per minute (9 inches per minute)
- Electrode wire diameter is 0.47625 cm (3/16 inches)
- Ambient temperature = 24.4 degrees C

Figure 4.3 Temperature on surface of uninsulated 0.635 cm and 2.54 cm (0.25 and 1 inch) thick mild steel plates at a distance of 0.5 cm from weld centerline

The combined effects of the aforementioned simplifications on computed results can not be quantified. However, the assumptions have been justified, and the model validated with experimental results. Consequently, the model can be used to predict insulation effects on wet SMA welds.

33

4.5 Computed Results

Figure 4.4 shows the computed effect of surface insulation on a wet SMA weld. Ideal insulation has been placed over the entire surface of the plate with the exception of the flux strip. Ideal insulation is defined as the imposition of a zero flux boundary condition.

- Arc Power = 5000W and arc efficiency = 0.53
- Travel speed = 22.86 cm per minute (9 inches per minute)
- Electrode wire diameter is 0.47625 cm (3/16 inches)
- Ambient temperature = 24.4 degrees C

Figure 4.4 Temperature on fully insulated 0.635 cm (0.25 inch) thick mild steel plate surface at a distance of 0.5 cm from weld centerline

Figure 4.4 represents ideal conditions which can not be achieved in practice. No insulation scheme will have zero conductivity. However, it is instructive in that it

34

demonstrates that surface thermal insulation could have a substantial effect on wet weld HAZ cooling. The ideally insulated plate attains a peak HAZ surface temperature 150% higher than the uninsulated plate, and the former HAZ cools to ambient temperature more gradually than the latter. The critical cooling range for martensite formation is 800 to 500 degrees C. The uninsulated weld HAZ peak temperature barely attains the lower limit of the critical range, while the insulated HAZ peak temperature exceeds the upper limit. Consequently, critical cooling rate comparisons between these two simulated welds can not be made. However, this computation indicates that the insulated HAZ surface temperature is substantially higher than that of the uninsulated HAZ until ten seconds after arc passage.

Figure 4.4 simulates a drag-consumption weld pass. The arc is "dragged" straight along the weld line with minimal manipulation. In this case the insulation can be abutted almost directly against the welding arc line. In the case of figure 4.4, the insulation begins 0.024 cm from weld centerline, thereby allowing electrode passage but no manipulation. If weld puddle weave manipulation is required, the insulation would have to be backed away from the weld line. Figure 4.5 on page 36 shows the result of moving the surface insulation so that insulation commences at a distance of 0.5 cm from the weld centerline to allow for puddle manipulation.

Comparison of figures 4.4 and 4.5 demonstrates the importance of placing surface insulation close to the weld. The effects of moving insulation away from the weld are a decrease in peak temperature and an increase in cooling rate. These are logical results based on the form of the assumed relationship for convective heat loss (equation {4.14}). Temperature differences between the plate surface and the surrounding water will be largest close to the heat source. Therefore, convective heat losses will be greatest closer to the arc. Insulation placed close to the arc will thus be more effective in reducing convective heat loss—and thereby increasing peak temperature and slowing the cooling rate—than insulation further from the arc.

Figure 4.6 (page 37) compares the effects of surface insulation with insulation placed on the back of a quarter inch thick plate. For this thickness, convective heat loss from the back of the plate is still significant, although far less important than convective losses from the surface.
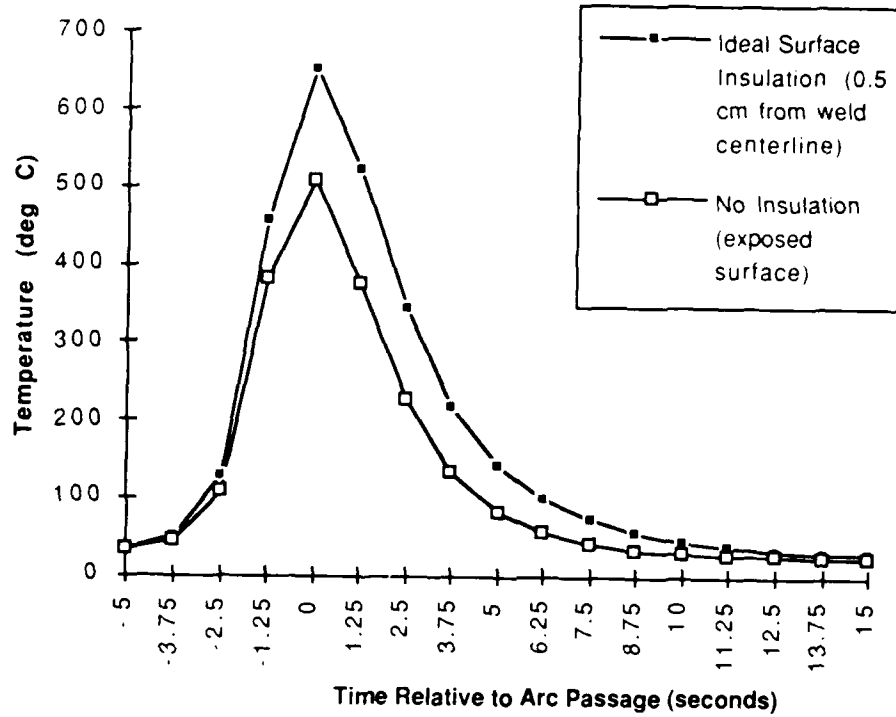
- Arc Power = 5000W and arc efficiency = 0.53
- Travel speed = 22.86 cm per minute (9 inches per minute)
- Electrode wire diameter is 0.47625 cm (3/16 inch)
- Ambient temperature = 24.4 degrees C

Figure 4.5 Temperature on partially insulated 0.635 cm (0.25 inch) thick mild steel plate surface at a distance of 0.5 cm from weld centerline (insulation starts 0.5 cm from weld centerline)
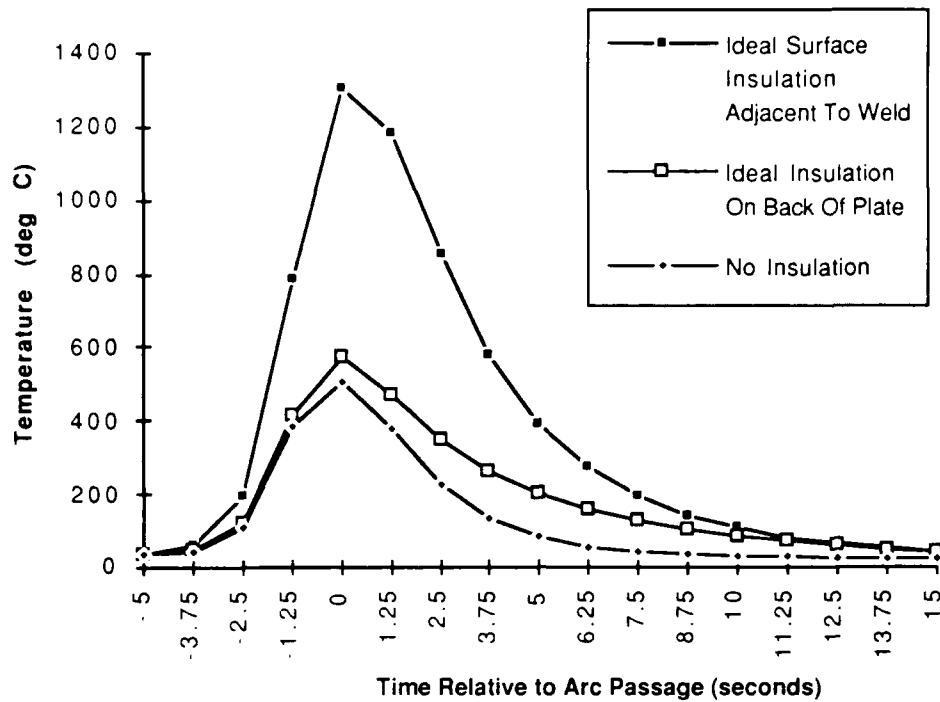
Figure 4.6 Temperature on 0.635 cm (0.25 inch) thick mild steel plate surface at a distance of 0.5 cm from weld centerline

●Arc Power = 5000W and arc efficiency = 0.53
●Travel speed = 22.86 cm per minute (9 inches per minute)
●Electrode wire diameter is 0.47625 cm (3/16 inch)
●Ambient temperature = 24.4 degrees C

As plate thickness is increased, back side convective losses should decrease. When the semi-infinite body thickness of approximately 0.75 inches is reached, there will be no convection from the back of the plate according to the hypothesis of chapter 3. This hypothesis is supported by the data presented in figure 4.7. Cooling rate and peak temperature for a one-inch-thick plate are unaffected by the use of back side insulation.
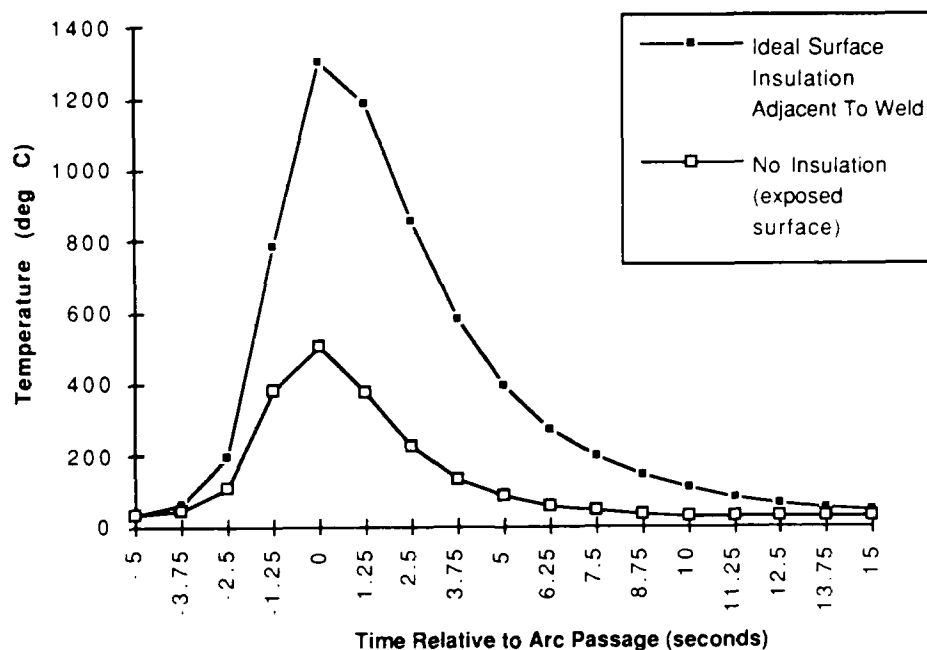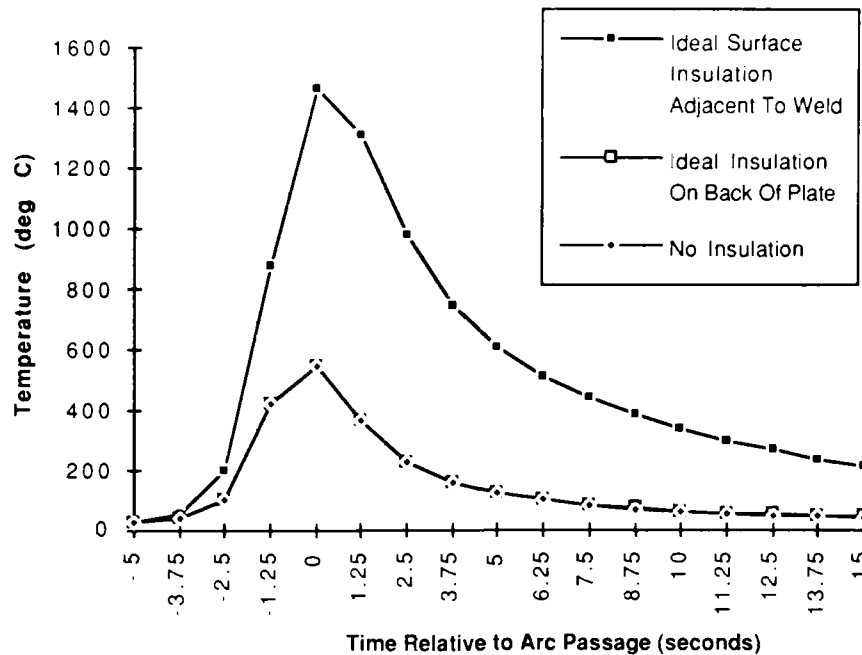
- Arc Power = 5000W and arc efficiency = 0.53
- Travel speed = 22.86 cm per minute (9 inches per minute)
- Electrode wire diameter is 0.47625 (3/16 inch)
- Ambient temperature = 24.4 degrees C

**Figure 4.7 Temperature on 2.54 cm (1 inch) thick mild steel plate surface
at a distance of 0.5 cm from weld centerline**

Computational modeling has demonstrated that placement of surface insulation close to the arc of a wet SMA weld could significantly increase the peak temperature and decrease the cooling rate on the surface of the weld HAZ.

4.6 Modeling Conclusions

The increase in peak temperature and the cooling rate reduction of a wet SMA weld HAZ surface—demonstrated by the computational model—illustrate the potential of the surface insulation method for improving wet weld quality. These changes in weld

cooling parameters could reduce the amount of martensite formed in wet weld HAZs, lessen hydrogen embrittlement and oxygen and slag induced porosity, reduce residual tensile stresses, and cause the formation of more concave weld beads.

In addition to demonstrating the potential of surface insulation, computational results have also shown a major limitation. Insulation must be placed close to the arc for optimum results. Consequently, puddle manipulation will be limited, but more importantly, the insulation material will have to be capable of withstanding extreme temperatures. Appropriate insulation materials must maintain low conductivity and be thermally stable at temperatures exceeding 1100 degrees C. Materials with such properties may not be readily available, or may be expensive or difficult to use (for reasons such as low ductility).

The computer model incorporated ideal insulation. Placement of actual insulation materials on the surface of the model would have required reducing the number of elements used in modeling the plate. Nekton is limited to 40 elements for 3-D models and 40 elements were used in the plate model to obtain maximum accuracy. The result of removing plate elements to model insulation materials would have been a different cooling curve in which the changes could not be attributed specifically to either the insulation or the change in plate modeling parameters. Ideal insulation was thus used based on modeling considerations. With the exception of a perfect vacuum (which would be impractical to create in the water) insulation with zero conductivity does not exist. (Even if *material* with zero conductivity could be acquired, the insulation to plate surface interface would not be perfect and there would be heat transferred into the interface). Consequently, the computed results represent an upper bound of the effects of insulation material. Actual insulation materials and imperfect interfaces encountered in practice will be less effective in reducing weld quenching.

Modeling has demonstrated an insulation-induced reduction in surface HAZ cooling. The surface is the area of the HAZ which is most rapidly cooled because of direct exposure to water. It is also the most likely location for crack initiation because of separation from the plate neutral axis and exposure to a corrosive environment. It is assumed that insulation will have less of an effect on the cooling rate of internal sections of the HAZ where quenching is not as severe.

Computational modeling has served to demonstrate the potential of surface insulation. Laboratory tests must be conducted to prove its effectiveness.

CHAPTER 5. EXPERIMENTAL PROCEDURE

A series of experimental welds were made in the Welding Systems Laboratory of MIT's Ocean Engineering Department to determine the effects of surface insulation on wet SMA welds. Welds were made manually with the base plates submerged in a small reservoir filled with water and the welder standing outside the reservoir welding through the air-water interface. Surface hardness testing and microscopic weld examination were used to evaluate the effects of insulation on the welds.

At the outset of the experimental phase of this research, attempts were made to use an automated welding system to make the experimental welds. It was thought that by using an automated process, the parameters affecting heat input—such as arc size and travel rate, weld current and voltage—could be held constant for all welds. Uninsulated and fully insulated welds could then have been made with equivalent heat inputs, and subsequently compared to evaluate the effect of insulation. This methodology could not be used for two reasons. First, the only automated welding system which was available for experimental use was the laboratory *Jetline Engineering* GTAW system. This particular system was designed to control the relatively low arc currents and voltages (i.e., 75 amps and 10 volts) used in GTA welding. The system was modified to weld with a SMAW electrode. However, testing demonstrated that the automation system could not consistently control the arc currents and voltages required for wet SMA welding (150 amps and 29 volts). Equivalent heat input profiles could not be obtained from one test weld to another. Second, the base plate travel (carriage) subassembly of the *Jetline Engineering* system had too small a track width to move a water reservoir large enough to maintain an approximately constant water temperature during welding. Ambient water temperature increases of up to 20% were measured during automated welding trials with a reservoir small enough to be used with the *Jetline Engineering* system. An increase in ambient water temperature during welding could reduce weld cooling rates. This effect would never be present in the virtually infinite heat sinks (i.e., oceans and rivers) in which wet SMAW is actually performed. To accurately evaluate the effect of insulation under actual welding conditions, ambient water temperature must be kept constant during welding. Consequently, a reservoir larger than that which could be moved by the automated system had to be used. For these reasons it was decided early in the experimental phase that welds would have to be made manually.

5.1 Description of the Experimental Procedure and Equipment

Changes in travel rate and arc length inherent in manual welding produce variations in heat input. Thus—even with stringent control of other experimental parameters—differences between uninsulated and fully insulated manual welds could not be positively attributed to insulation, because differences could arise from varying heat input profiles. Consequently, a procedure was developed that separated the effects of variations in heat input from insulation effects. Welds were insulated only along one side and the remaining side was left uninsulated. Each weld, with it's specific heat input and insulation configuration, could then be tested independently to evaluate the effects of insulation.

A welding jig was constructed that consisted of a base plate platform with securing clamps, electrode guides, insulation clamping screws, and a ground attachment point. Base plates of varying thickness could be clamped into the jig. Insulation materials were then clamped onto one side of the base plate with the edge of the insulation closest to the welding line positioned directly under the electrode guide so that all welds were made with insulation adjacent to the weld line. (Control welds were made with no insulation on either side of the base plate to establish baselines for the hardness testing phase of the experimental procedure). The welding jig and base plate were then placed in a reservoir containing 35.5 liters of fresh water, and the welding power supply ground was attached to the jig/base plate assembly. Welds were made using the electrode guides to ensure that the arc was directly adjacent to the insulation material during welding. Bead-on-plate welds were made because of the simplicity of this weld geometry. Figure 6.1 shows a typical experimental set-up prior to placement of the jig in the welding reservoir.
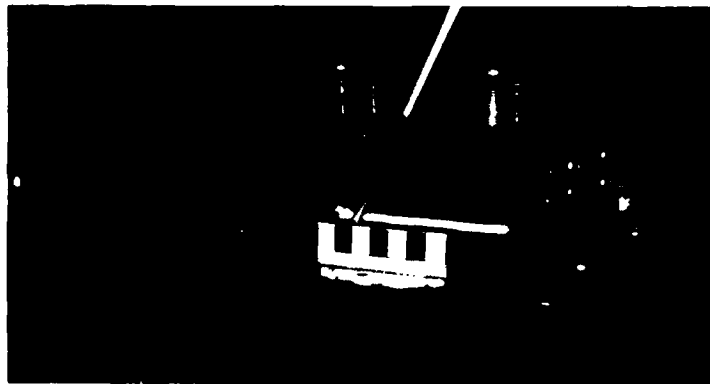
Figure 5.1 Welding Jig with Base Plate and Insulation

41

Three types of insulation were tested. All were fabrics woven from 3M Nextel™ 312 alumina-boria-silica fibers. The primary difference between the fabrics that were used was permeability. The Nextel fabrics were chosen because of their stability when exposed to high temperatures (no shrinkage or strength loss after continuous exposure of up to 1204 degrees C) and because of their low thermal conductivity (approximately 0.16 W/m C at 650 degrees C) [13]. (In comparison, the thermal conductivity of fabrics woven from asbestos (inorganic silica) fibers is approximately 0.17 W/m C at 650 degrees C [14].) High temperature stability allowed the insulation to be placed adjacent to the weld line, thereby optimizing it's effect on heat flow as discussed in section 4.5. Low thermal conductivity reduces through-insulation heat loss to the environment and is therefore of primary importance in reducing weld cooling rates. Additionally, the Nextel fabrics are pliable, can be formed to interface with any geometry, and are therefore practical insulating materials. Table 5.1 lists the properties of the three Nextel fabrics that were tested.

Table 5.1 Insulation Fabric Properties [13]

Fabric Style	Thickness per Ply (mm)	Weave Type	Air Permeability (1) $\left[\dfrac{m^3}{m^2 \cdot min} \right]$
AF-62	0.81	Double Layer	38
AF-40	1.27	5 Harness Satin	11.6
AB-22 (filter bag)	0.56	5 Harness Satin	5.3

(1) At constant pressure differential equal to 0.5 inches of water

A *Miller Synchrowave 350* welding machine set for direct current straight polarity was used as a power source. Welding current was 150 amps. Open circuit voltage was 57.6 volts and average arc voltage during welding was 29 volts. All welding was performed with *BROCO Softouch* E70XX 1/8 inch diameter wet welding electrodes.

Temperature measurements were made in the welding reservoir immediately before, during, and upon completion of welding. Measurements were made at two positions, one at the edge of the plate being welded, and the other at a location in the reservoir removed from the welding site. K-type thermocouples (with a temperature measurement range of -200 to 1370 deg. C) connected to a calibrated *OMEGA RD-103-AR* chart recorder were used to make the temperature measurements. All welds were

timed, and bead length and average bead width recorded. Experimental weld parameters are presented in table 5.2.

Table 5.2 Experimental Weld Parameters (1)

Weld No.	Bead Lgth/Avg Bead Width cm/cm	Travel Rate (cm/s)	Base Metal (2)	Reservoir Temp. Prior to Welding (deg. C)	Reservoir Temp. Increase During Welding (deg. C) (3)	Insulation (8 plys applied to 1 side of weld for MS, 4 plys to both sides for HTS)
Control 1	13.2/0.5	0.73	MS	22.9	0.1	N/A
MS1	12.5/0.5	0.65	MS	22.9	0.2	AF-40
MS2	9.2/0.5	0.56	MS	21.3	0.0	AF-40
MS3	12.7/0.5	0.74	MS	15.3	0.0	AF-40
MS4	13.0/0.5	0.74	MS	18.6	0.2	AF-40
MS5	13.2/0.5	0.73	MS	20.7	0.1	AF-40
Control 2	12.0/0.4	0.71	HTS	23.9	0.1	N/A
HTS1	13.0/0.4	0.72	HTS	24.0	0.1	AB-22

(1) All welds made with *BROCO Softouch* E70XX 1/8 inch diameter wet welding electrodes with 150 amp welding current and 29 volt average arc voltage. Base plate dimensions were 6 inches in the direction of the weld line and 4 inches perpendicular to the weld for MS, and 5.5 and 8 inches respectively for HTS.

(2) CE of MS (ASTM A36 mild steel) = 0.285 and CE of HTS (DH-36 High Tensile Strength Steel) = 0.41. Base plate thicknesses were 0.25 inch for MS and 0.5 inch for HTS.

(3) From average of temperatures at both thermocouple locations

5.2 Evaluation of Experimental Welds

According to Okumura and Yurioka of the Nippon Steel Corporation, "The hardness of heat affected zones is the most basic property in assessing the weldability of steels" and, "HAZ hardness tests are generally conducted as one of the welding procedure approval tests" [15] As discussed in section 2.1 of this thesis, HAZ hardness is directly related to the weld cooling rate. MIT welding engineering professor K. Masubuchi has stated that hardness testing is a more reliable method of determining the effects of various

weld parameters on the cooling rate than direct temperature measurement, because of the difficulty of obtaining accurate temperature readings close to a welding arc. Consequently, the primary means used in this experiment to evaluate the effects of surface insulation on weld cooling rates was HAZ hardness testing. Hardness was measured on all mild steel welds with an *Acco Wilson* Model 4JR Rockwell Hardness Tester. Welds were not ground prior to hardness testing because grinding heat input would have had a non-measurable effect on surface hardness. In addition to hardness testing, the HTS welds, and one mild steel weld were sectioned, polished, acid etched, and visually inspected using a *Hirox Co.* LTD. Model KN-2200 MD2 fiber optic microscope.

CHAPTER 6. EXPERIMENTAL RESULTS

More than fifty trial welds were made on mild steel plates during the initial phase of the manual welding experiment. The purpose of these welds was to practice the welding technique so that welds with relatively consistent travel rate and bead profile could be attained. At first, the majority of the welds had longitudinally varying bead profiles. Four of these trial welds (two of which had been insulated with AF-62 fabric and two with AF-40) were tested for hardness. The standard deviations of the hardness values were high because of bead profile irregularities. However, the results did indicate that the less permeable AF-40 fabric provided better insulation than AF-62. This result is intuitive. The purposes of insulation are to provide a thermal resistance and to displace water from the plate surface so as to limit convective heat losses. The less permeable insulation was more effective in displacing water from the plate surface, limiting convection, and thereby reducing the weld cooling rate. Consequently, welds made with AF-40 insulation showed a slight statistically relevant reduction in surface hardness as compared to the welds insulated with AF-62. Because of bead irregularities, measured hardness values for these welds were considered unsuitable for use as experimental data. However, the conclusion that AF-40 was a more effective insulating material than AF-62 was assumed to be valid, and further tests were performed solely with the less permeable AF-40 and AB-22 materials. (AB-22 became available after mild steel welding had been completed, and was therefore used only in the subsequent HTS phase of the experiment).

The Nextel fabrics proved to be quite durable. They were capable of being used repeatedly, and even when subjected directly to the submerged arc, they did not melt.

With practice, welding travel rate and weld bead profile consistency were attained. Eight "experimental" welds were then made. Six were made on 0.25 inch thick 0.285 CE mild steel plate. These mild steel welds consisted of one control weld, which was not insulated, and five welds that were insulated on one side of the weld line. After completion of the mild steel testing phase, two experimental welds were made on 0.5 inch thick 0.41 CE HTS. This grade of steel was chosen because recent tests conducted by the Naval Sea Systems Command had found underbead cracking in all wet welds made on plates with CEs greater than 0.40. Welding parameters for all experimental welds were presented previously in table 5.2. A photographs of two typical experimental mild steel welds is shown in figure 6.1.

Figure 6.1 Photographs of Typical Experimental Mild Steel Welds

6.1 Results From Hardness Testing and Visual Inspection of Welds Made on Mild Steel Plates

Hardness testing results from the mild steel plate welds are presented in tables 6.1 through 6.3. In each case, ten hardness readings were taken on each side of the weld line. The weld crown was used as a lateral reference because of the relative ease of identifying the apex of the crown. (The exact location of the weld toe would have been more difficult

Table 6.1 Hardness Testing Results from Mild Steel Control Weld and MS1

Control

Sample	Rockwell A Hardness (1/4 inch from weld crown)		χ^2 ((Sample Mean-Sample Value)^2)	
	Side 1	Side 2	Side 1	Side 2
1	50.0	34.0	5.76	97.02
2	45.0	41.0	6.76	8.12
3	52.0	47.0	19.36	9.92
4	51.5	42.0	15.21	3.42
5	48.0	39.0	0.16	23.52
6	42.0	38.0	31.36	34.22
7	45.5	36.5	4.41	54.02
8	41.5	54.0	37.21	103.02
9	52.0	57.0	19.36	172.92
10	48.5	50.0	0.81	37.82

$\overline{X}_1$ (Smpl Mean)	$\overline{X}_2$ (Smpl Mean)	s_1 (Smpl Std Dev)	s_2 (Smpl Std Dev)
47.60	43.85	3.75	7.38

σ	t	t(0.60)	t(0.70)
6.17	0.27	0.26	0.54

MS1

Sample	Rockwell A Hardness (1/4 inch from weld crown)		χ^2 ((Sample Mean-Sample Value)^2)	
	Uninsulated Side	Insulated Side	Uninsulated Side	Insulated Side
1	45.0	28.5	2.72	78.32
2	47.0	36.5	0.12	0.72
3	46.5	36.5	0.02	0.72
4	46.0	37.0	0.42	0.12
5	47.0	46.0	0.12	74.82
6	44.0	42.5	7.02	26.52
7	48.5	45.0	3.42	58.52
8	43.5	24.5	9.92	165.12
9	49.0	33.5	5.52	14.82
10	50.0	43.5	11.22	37.82

$\overline{X}_U$ (Smpl Mean)	$\overline{X}_I$ (Smpl Mean)	s_U (Smpl Std Dev)	s_I (Smpl Std Dev)
46.65	37.35	2.01	6.76

σ	t	t(0.75)	t(0.80)
5.26	0.79	0.70	0.88

Table 6.2 Hardness Testing Results from Welds MS2 and MS3

MS 2

Sample	Rockwell A Hardness (1/4 inch from weld crown) Uninsulated Side	Insulated Side	χ^2 ((Sample Mean-Sample Value)^2) Uninsulated Side	Insulated Side
1	41.5	30.0	21.16	68.89
2	45.0	35.0	1.21	10.89
3	45.0	42.0	1.21	13.69
4	45.5	44.0	0.36	32.49
5	50.5	44.5	19.36	38.44
6	47.5	27.5	1.96	116.64
7	43.0	40.0	9.61	2.89
8	48.5	43.5	5.76	27.04
9	49.5	33.0	11.56	28.09
10	45.0	43.5	1.21	27.04

$\overline{X}_U$ (Smpl Mean)	$\overline{X}_I$ (Smpl Mean)	s_U (Smpl Std Dev)	s_I (Smpl Std Dev)
46.10	38.30	2.71	6.05

σ	t	t(0.75)	t(0.80)
4.94	0.71	0.70	0.88

MS 3

Sample	Rockwell A Hardness (1/4 inch from weld crown) Uninsulated Side	Insulated Side	χ^2 ((Sample Mean-Sample Value)^2) Uninsulated Side	Insulated Side
1	48.5	40.0	0.56	6.00
2	50.0	46.0	5.06	12.60
3	50.5	41.5	7.56	0.90
4	44.0	40.0	14.06	6.00
5	47.0	46.5	0.56	16.40
6	45.5	40.0	5.06	6.00
7	51.0	40.0	10.56	6.00
8	46.0	44.0	3.06	2.40
9	47.5	43.5	0.06	1.10
10	47.5	43.0	0.06	0.30

$\overline{X}_U$ (Smpl Mean)	$\overline{X}_I$ (Smpl Mean)	s_U (Smpl Std Dev)	s_I (Smpl Std Dev)
47.75	42.25	2.16	2.40

σ	t	t(0.80)	t(0.90)
2.41	0.98	0.88	1.38

Table 6.3 Hardness Testing Results from Welds MS4 and MS5

MS 4

Sample	Rockwell A Hardness (1/4 inch from weld crown)		χ^2 ((Sample Mean-Sample Value)^2)	
	Uninsulated Side	Insulated Side	Uninsulated Side	Insulated Side
1	42.0	44.5	11.90	3.24
2	41.5	41.5	15.60	1.44
3	45.0	39.0	0.20	13.69
4	46.0	41.0	0.30	2.89
5	48.0	45.5	6.50	7.84
6	49.0	40.0	12.60	7.29
7	44.0	40.0	2.10	7.29
8	46.0	46.0	0.30	10.89
9	46.0	46.5	0.30	14.44
10	47.0	43.0	2.40	0.09

$\overline{X}_U$ (Smpl Mean)	$\overline{X}_I$ (Smpl Mean)	s_U (Smpl Std Dev)	s_I (Smpl Std Dev)
45.45	42.70	2.29	2.63

σ	t	t(0.60)	t(0.70)
2.60	0.47	0.26	0.54

MS 5

Sample	Rockwell A Hardness (1/4 inch from weld crown)		χ^2 ((Sample Mean-Sample Value)^2)	
	Uninsulated Side	Insulated Side	Uninsulated Side	Insulated Side
1	46.0	34.0	0.12	31.36
2	49.0	38.5	7.02	1.21
3	46.5	41.0	0.02	1.96
4	48.0	44.5	2.72	24.01
5	50.0	45.0	13.32	29.16
6	43.5	35.0	8.12	21.16
7	46.0	41.5	0.12	3.61
8	45.0	43.5	1.82	15.21
9	45.5	35.0	0.72	21.16
10	44.0	38.0	5.52	2.56

$\overline{X}_U$ (Smpl Mean)	$\overline{X}_I$ (Smpl Mean)	s_U (Smpl Std Dev)	s_I (Smpl Std Dev)
46.35	39.60	1.99	3.89

σ	t	t(0.80)	t(0.90)
3.26	0.93	0.88	1.38

to specify). Hardness was measured at a lateral offset of 1/4 inch from the weld crown because this was the closest that the weld could be approached with the indenter tip of the testing device without the indenter bale impacting the weld bead reinforcement. From visual inspection it appeared that measurements taken at the 1/4 inch offset distance were within the weld HAZ. Hardness readings were taken in pairs (one reading on the insulated side and one on the uninsulated side) at random locations along the weld. The Rockwell A testing scale was chosen because it provided readings close to 50% scale deflection for the samples being evaluated.

To determine the statistical significance of the results the "Student's t" analysis was used. This analysis is valid for sample sizes of less than 30 with an assumed normal distribution [16]. The t analysis is described in the following paragraphs .

First, the sample mean ($\overline{X}$) from each population (i.e., uninsulated side or insulated side) is computed. Second, the sample standard deviation (s) is computed for each population. The statistic σ is then calculated as shown in equation {6.1}.

$$\sigma = \sqrt{\frac{N_1 s_1^2 + N_2 s_2^2}{N_1 + N_2 - 2}} \qquad \{6.1\}$$

Where:

N_1, N_2 are the number of samples taken in populations 1 and 2
s_1, s_2 are the sample standard deviations of populations 1 and 2

Finally, the statistic t is computed using equation {6.2}.

$$t = \frac{\overline{X}_1 - \overline{X}_2}{\sigma\sqrt{1/N_1 + 1/N_2}} \qquad \{6.2\}$$

The t statistic represents the significance level of the difference in the sample means of the two populations. Hence, a high value of t (a high significance level) indicates that there is a high probability that a difference in sample means is the result of sampling from two physically distinct populations (i.e., a brittle uninsulated side and a ductile insulated side). A low value of t (low significance level) is indicative of the samples having been drawn from the same overall population, with any difference in sample means being the result of measurement standard deviations. The latter case would be expected for control welds since no physical difference should exist in the hardness values measured on either side of these welds. Significance levels (i.e., t(0.90), t(0.80))

are tabulated for different degrees of freedom. (The number of degrees of freedom of a statistic is defined as the sample size minus the number of population parameters which must be estimated from sample populations. In the case of t, the number of degrees of freedom = N-1, where N is the sample size [16]). It is these significance levels which are tabulated—along with the computed values of t—in tables 6.1 through 6.3.

The results of control weld testing presented in table 6.1 demonstrate that there is approximately a 10% measurement error inherent in the experimental and testing procedures and sample sizes (N = 10) that were used. (t ≈ t(0.60), signifying a 60% significance level for the difference in mean sample hardness values between sides 1 and 2. Since this is a control weld, we would expect t ≈ t(0.50), a 50% or random significance level. Thus the measurement error can be approximated as the difference between these significance levels which is 10%). The primary methods for reducing measurement error are to reduce sample standard deviation (σ) and increase sample size.(N) The standard error associated with a sample mean ($\sigma_{\bar{x}}$) is given by equation {6.3} [16].

$$\sigma_{\bar{x}} = \frac{\sigma}{\sqrt{N}} \qquad \{6.3\}$$

Sample standard deviation values were inherent to the manual welding process and could not be reduced without improving the consistency of heat input along the length of the weld. Additionally, since $\sigma_{\bar{x}}$ is proportional to the inverse square root of the sample size, a sample size of N = 100 would theoretically have been required to reduce the measurement error from 10% to approximately 3-4%. Sample sizes of 100 would not have been practical given the lengths of the welds being tested. Consequently, 10% measurement errors are associated with all hardness values reported in this thesis.

The data presented in tables 6.1 through 6.3 shows that all five insulated mild steel welds demonstrated decreased surface HAZ hardness on the insulated sides of the weld beads. Furthermore, in addition to this insulation effect being demonstrated in *all five* welds, the results are statistically significant even after measurement error has been considered. Specifically, the average significance level for the reduction in surface hardness due to insulation in welds MS1 through MS5 is t(0.77). This is 17% higher than the significance level of the control weld. Figures 6.2 and 6.3 graphically depict the measured mean hardness differences between insulated and uninsulated sides of all mild steel welds, and the absolute relevant hardness differences between sides for welds MS1 through MS5, respectively.
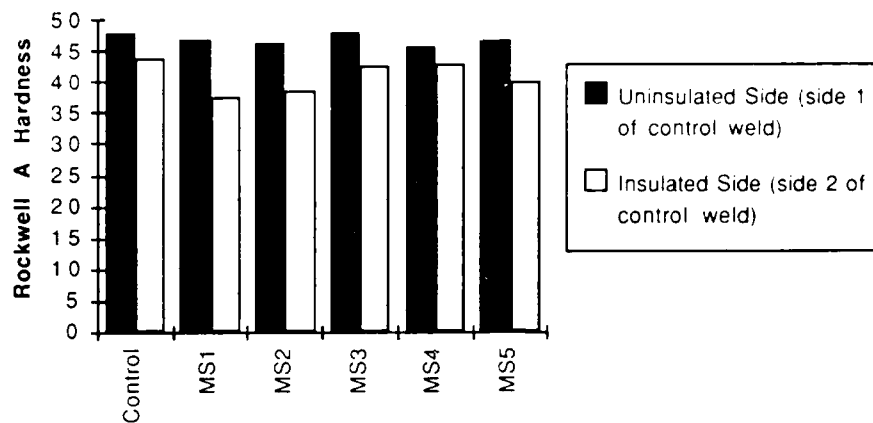
Figure 6.2 Comparison of Mean Hardness Values for Mild Steel Test Welds
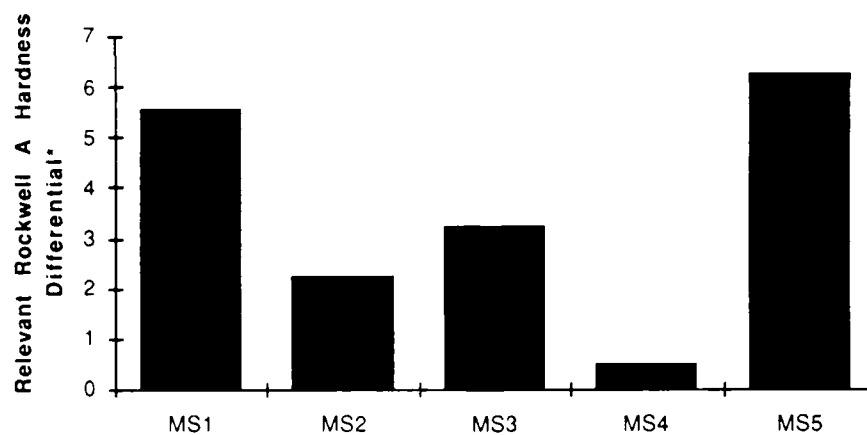
* |((Uninsulated Side Sample Mean Hardness)-(Insulated Side Sample Mean Hardness))-
(Hardness Difference Between Control Weld Sides 1 and 2)|

Figure 6.3 Experimentally Relevant Higher Mean Hardness Values of the
Uninsulated Sides of Mild Steel Welds 1 through 5

It is important to note that one-sided surface insulation would theoretically be less effective in reducing weld cooling rates—and surface HAZ hardness—than two sided or full insulation, because of asymmetric heat flow in the former. The weld centerline is not a symmetry plane, and greater heat flux through the less thermally resistant uninsulated side would be expected. The result would be a faster overall cooling rate for a weld insulated on one side than for a fully insulated weld.

Visual inspection of the sectioned mild steel weld (MS 5) was inconclusive. No difference in HAZ shape between the insulated and uninsulated sides was evident at a magnification level of 10 X.

6.2 Results From Visual Inspection of Welds Made on High Strength Steel Plates

Microscopic examination of the two 0.41 CE HTS welds revealed differences in the fusion line between the uninsulated and fully insulated welds. At 10 X magnification the uninsulated weld fusion line was traversed by numerous perpendicular underbead cracks. The fusion line of the insulated weld was smooth, and underbead cracks were not apparent. This observation was confirmed by an AWS certified welding inspector, Mr. Robert Murray of the Naval Sea Systems Command. Mr Murray stated that in previous wet welding tests of plates exceeding 0.40 CE, underbead cracking had been found in all welds. This form of cracking can be attributed to rapid contraction of the HAZ as a result of weld quenching.

No definitive conclusions can be made from the examination of two welds. However the results of visual examination of the HTS welds, coupled with the hardness testing results from the mild steel welds, suggest that surface thermal insulation may indeed slow the cooling rates of wet SMA welds as predicted by computational modeling. Further, more controlled testing is required to definitively prove this hypothesis, and to accurately quantify the effect of insulation-induced quenching reduction on weld ductility and strength.

CHAPTER 7. CONCLUSION

This thesis has demonstrated both computationally and experimentally that thermal insulation can be used to reduce the quenching rate and thereby improve the quality of wet SMA welds. Thermal insulation has been shown to be practically and economically feasible. Placement of static insulation during fit-up will have only a marginal impact on weld set-up times. Commercially available, pliable, re-usable, non-toxic, and relatively inexpensive insulation materials (Nextel AB-22 fabric is sold as woven seamless tubing with a 4 5/8 inch outside diameter at a cost of $40.40 per linear foot) have been tested in the laboratory with satisfactory results. However, because of limitations in experimental capabilities (specifically the use of the author, a non-coded welder, to make manual experimental welds) the full potential of this technology advance has not been demonstrated.

As a result of this initial research, the U.S. Navy has initiated a program to evaluate more thoroughly the effect of insulation on wet SMA welds. The Navy plans to use AWS coded wet welders/divers to perform butt welds while fully submerged in a large testing tank. These welders will weld at pre-specified travel rates with tightly controlled welding parameters. Heat input consistency between welds will allow testing and comparison of both fully insulated (insulation on both sides of the joint) and uninsulated joints. Welds will be destructively bend-tested to directly measure ductility and strength. Additionally, research will be performed to determine if better insulation materials than the Nextel fabrics—lower conductivity and permeability, and improved thermal stability and pliability—are commercially available. All research and testing will be carried out under the provisions of the Massachusetts Institute of Technology, Technology Licensing Office, through which a patent application has been filed with the U.S. Patent Office (case number 6107) entitled "Thermal Insulation of Wet Shielded Metal Arc Welds."

Results from the Navy testing program could convincingly demonstrate the viability of thermally insulated wet welds, thereby leading to improvements in wet SMA weld quality, and allowing wet SMAW to be used on a wider range of materials in both commercial and military applications.

REFERENCE LIST

1. American Welding Society. *Specification for Underwater Welding*. AWS. Miami. 1982.

2. Tsai, C.L. *Parameteric Study on Cooling Phenomena in Underwater Welding*. Massachusetts Institute of Technology. 1977.

3. Masubuchi, K., and D.C. Martin. *Mechanisms of Cracking in HY-80 Steel Weldments*. Welding Journal Research Supplement. August 1962.

4. Masubuchi, K., et al. *TMCP Steels for Construction and Repair of Marine Structures*. 1992.

5. ARCAIR CO. *ARCAIR Instruction Manual for Underwater Cutting and Welding*. 1982.

6. West, T.C., G. Mitchell, and E. Lindberg. *Wet Welding Evaluation for Ship Repair*. Welding Journal, August 1990: 46-56.

7. Masubuchi, K., A.B Gaudiano and T.J. Reynolds. *Technologies and Practices of Underwater Welding*. Underwater Welding Conference Proceedings, 1983: 49-70.

8. Stalker, A.W. *Welding Institute Research on Underwater Welding*. Underwater Welding for Offshore Installations. The Welding Institute. Abington Hall. 1977.

9. Bouaman, H., and J. Haverhals. *Underwater Welding With Covered Electrodes*. Lastechbik, 1971: Vol. 37, No. 12, 219-226.

10. Tsai, C.L. et al. *Development of New Improved Techniques for Underwater Welding*. MIT Sea Grant Program. 1977: MITSG 77-9.

11. Satoh, K. et al. *Study on Improvement of Locally Drying Underwater Welding Joint by Retarded Cooling Method*. Journal of the Japanese Welding Society, August 1982: 665-672.

12. Zienkiewicz, O.C., *The Finite Element Method in Structural and Continuum Mechanics*. McGraw Hill. London. 1968.

13. Nextel™ 312 Woven Fabrics Product Bulletin. 3M Corporation, St. Paul, Minnesota. 1992.

14. Turner, W.C., and J.F. Malloy. *Thermal Insulation Handbook*. McGraw Hill Inc. NY, NY. 1981.

15. Okumura, M, and N. Yurioka. *HAZ Hardness Tests for Evaluation of Steel Weldability*. Nippon Steel Corporation Steel Research Laboratories. May 1992.

16. Spiegel, M.R. *Theory and Problems of Statistics* 2 ed. McGraw Hill Inc. NY, NY. 1992.

APPENDIX A

FORTRAN code used to create an uninsulated 40-element three-dimensional geometric model (NEKTON . rea File).

```
****** PARAMETERS *****
2.700000      NEKTON VERSION
3 DIMENSIONAL RUN
53 PARAMETERS FOLLOW
1.00000            DENSITY
1.00000            VISCOS
0.000000E+00       BETAG
0.000000E+00       GTHETA
0.000000E+00       PGRADX
0.000000E+00       FLOWRATE
0.364000E+07       RHOCP
35.9100            CONDUCT
0.000000E+00       QVOL
30.0000            FINTIME
24.0000            NSTEPS
1.25000            DT
0.000000E+00       IOCOMM
0.000000E+00       IOTIME
0.000000E+00       IOSTEP
0.000000E+00       EQTYPE
0.000000E+00       AXIS
0.500000E-01       GRID
-1.00000           INTYPE
5.00000            NORDER
0.000000E+00       DIVERGENCE
0.100000E-03       HELMHOLTZ
0.000000E+00       NPSCAL
0.100000E-01       TOLREL
1.00000            TOLABS
0.250000           COURANT
2.00000            TORDER
0.000000E+00
0.000000E+00
0.000000E+00
0.000000E+00
0.000000E+00
0.000000E+00
0.000000E+00
0.000000E+00
0.000000E+00       XMAGNET
0.000000E+00       NGRIDS
0.000000E+00       NORDER2
0.000000E+00       NORDER3
0.000000E+00       NORDER4
0.000000E+00       NORDER5
0.000000E+00
0.000000E+00
0.000000E+00
0.000000E+00       FSDTFAC
0.000000E+00       IRSTART
0.000000E+00
0.000000E+00
0.140000           MIXLFAC
0.000000E+00
0.000000E+00
0.000000E+00       HISTEP
0.000000E+00       HISTIME
```

4 Lines of passive scalar data follow2 CONDUCT; 2RHOCP
1.00000   1.00000   1.00000   1.00000   1.00000

```
1.00000        1.00000        1.00000        1.00000
1.00000        1.00000        1.00000        1.00000        1.00000
1.00000        1.00000        1.00000        1.00000
         13  LOGICAL SWITCHES FOLLOW
         F       IFFLOW
T      IFHEAT
T      IFTRAN
F F F F F F F F F F F F IFNAV & IFADVC (convection in P.S. fields)
F F T T T T T T T T T T IFTMSH (IF mesh for this field is T mesh)
F      IFAXIS
F      IFSTRS
F      IFSPLIT
F      IFMGRID
F      IFMODEL
F      IFKEPS
F      IFMVBD
F      IFCHAR
0.119063 0.119063 -0.357188E-01 -0.178594E-01 XFAC,YFAC,XZERO,YZERO
**MESH DATA** 6 lines are X,Y,Z;X,Y,Z. Columns corners 1-4;5-8
40      3      40              NEL,NDIM,NELV
         ELEMENT    1  [  1A]    GROUP       0
0.000000E+00  0.476250E-02  0.476250E-02  0.000000E+00
0.000000E+00  0.000000E+00  0.238125E-02  0.238125E-02
0.000000E+00  0.000000E+00  0.000000E+00  0.000000E+00
0.000000E+00  0.476250E-02  0.476250E-02  0.000000E+00
0.000000E+00  0.000000E+00  0.238125E-02  0.238125E-02
2.540000E-02  2.540000E-02  2.540000E-02  2.540000E-02
         ELEMENT    2  [  1B]    GROUP       0
0.000000E+00  0.476250E-02  0.476250E-02  0.000000E+00
0.238125E-02  0.238125E-02  0.500000E-02  0.500000E-02
0.000000E+00  0.000000E+00  0.000000E+00  0.000000E+00
0.000000E+00  0.476250E-02  0.476250E-02  0.000000E+00
0.238125E-02  0.238125E-02  0.500000E-02  0.500000E-02
2.540000E-02  2.540000E-02  2.540000E-02  2.540000E-02
         ELEMENT    3  [  1C]    GROUP       0
0.238125E-01  0.285750E-01  0.285750E-01  0.238125E-01
0.000000E+00  0.000000E+00  0.238125E-02  0.238125E-02
0.000000E+00  0.000000E+00  0.000000E+00  0.000000E+00
0.238125E-01  0.285750E-01  0.285750E-01  0.238125E-01
0.000000E+00  0.000000E+00  0.238125E-02  0.238125E-02
2.540000E-02  2.540000E-02  2.540000E-02  2.540000E-02
         ELEMENT    4  [  1D]    GROUP       0
0.238125E-01  0.285750E-01  0.285750E-01  0.238125E-01
0.238125E-02  0.238125E-02  0.500000E-02  0.500000E-02
0.000000E+00  0.000000E+00  0.000000E+00  0.000000E+00
0.238125E-01  0.285750E-01  0.285750E-01  0.238125E-01
0.238125E-02  0.238125E-02  0.500000E-02  0.500000E-02
2.540000E-02  2.540000E-02  2.540000E-02  2.540000E-02
         ELEMENT    5  [  1E]    GROUP       0
0.476250E-02  0.952500E-02  0.952500E-02  0.476250E-02
0.000000E+00  0.000000E+00  0.238125E-02  0.238125E-02
0.000000E+00  0.000000E+00  0.000000E+00  0.000000E+00
0.476250E-02  0.952500E-02  0.952500E-02  0.476250E-02
0.000000E+00  0.000000E+00  0.238125E-02  0.238125E-02
2.540000E-02  2.540000E-02  2.540000E-02  2.540000E-02
         ELEMENT    6  [  1F]    GROUP       0
0.476250E-02  0.952500E-02  0.952500E-02  0.476250E-02
0.238125E-02  0.238125E-02  0.500000E-02  0.500000E-02
0.000000E+00  0.000000E+00  0.000000E+00  0.000000E+00
```

```
0.476250E-02   0.952500E-02   0.952500E-02   0.476250E-02
0.238125E-02   0.238125E-02   0.500000E-02   0.500000E-02
2.540000E-02   2.540000E-02   2.540000E-02   2.540000E-02
          ELEMENT    7   [  1G]    GROUP      0
0.952500E-02   0.142875E-01   0.142875E-01   0.952500E-02
0.000000E+00   0.000000E+00   0.238125E-02   0.238125E-02
0.000000E+00   0.000000E+00   0.000000E+00   0.000000E+00
0.952500E-02   0.142875E-01   0.142875E-01   0.952500E-02
0.000000E+00   0.000000E+00   0.238125E-02   0.238125E-02
2.540000E-02   2.540000E-02   2.540000E-02   2.540000E-02
          ELEMENT    8   [  1H]    GROUP      0
0.952500E-02   0.142875E-01   0.142875E-01   0.952500E-02
0.238125E-02   0.238125E-02   0.500000E-02   0.500000E-02
0.000000E+00   0.000000E+00   0.000000E+00   0.000000E+00
0.952500E-02   0.142875E-01   0.142875E-01   0.952500E-02
0.238125E-02   0.238125E-02   0.500000E-02   0.500000E-02
2.540000E-02   2.540000E-02   2.540000E-02   2.540000E-02
          ELEMENT    9   [  1I]    GROUP      0
0.142875E-01   0.190500E-01   0.190500E-01   0.142875E-01
0.000000E+00   0.000000E+00   0.238125E-02   0.238125E-02
0.000000E+00   0.000000E+00   0.000000E+00   0.000000E+00
0.142875E-01   0.190500E-01   0.190500E-01   0.142875E-01
0.000000E+00   0.000000E+00   0.238125E-02   0.238125E-02
2.540000E-02   2.540000E-02   2.540000E-02   2.540000E-02
          ELEMENT   10   [  1J]    GROUP      0
0.142875E-01   0.190500E-01   0.190500E-01   0.142875E-01
0.238125E-02   0.238125E-02   0.500000E-02   0.500000E-02
0.000000E+00   0.000000E+00   0.000000E+00   0.000000E+00
0.142875E-01   0.190500E-01   0.190500E-01   0.142875E-01
0.238125E-02   0.238125E-02   0.500000E-02   0.500000E-02
2.540000E-02   2.540000E-02   2.540000E-02   2.540000E-02
          ELEMENT   11   [  1K]    GROUP      0
0.190500E-01   0.238125E-01   0.238125E-01   0.190500E-01
0.000000E+00   0.000000E+00   0.238125E-02   0.238125E-02
0.000000E+00   0.000000E+00   0.000000E+00   0.000000E+00
0.190500E-01   0.238125E-01   0.238125E-01   0.190500E-01
0.000000E+00   0.000000E+00   0.238125E-02   0.238125E-02
2.540000E-02   2.540000E-02   2.540000E-02   2.540000E-02
          ELEMENT   12   [  1L]    GROUP      0
0.190500E-01   0.238125E-01   0.238125E-01   0.190500E-01
0.238125E-02   0.238125E-02   0.500000E-02   0.500000E-02
0.000000E+00   0.000000E+00   0.000000E+00   0.000000E+00
0.190500E-01   0.238125E-01   0.238125E-01   0.190500E-01
0.238125E-02   0.238125E-02   0.500000E-02   0.500000E-02
2.540000E-02   2.540000E-02   2.540000E-02   2.540000E-02
          ELEMENT   13   [  1M]    GROUP      0
0.285750E-01   0.333375E-01   0.333375E-01   0.285750E-01
0.000000E+00   0.000000E+00   0.238125E-02   0.238125E-02
0.000000E+00   0.000000E+00   0.000000E+00   0.000000E+00
0.285750E-01   0.333375E-01   0.333375E-01   0.285750E-01
0.000000E+00   0.000000E+00   0.238125E-02   0.238125E-02
2.540000E-02   2.540000E-02   2.540000E-02   2.540000E-02
          ELEMENT   14   [  1N]    GROUP      0
0.285750E-01   0.333375E-01   0.333375E-01   0.285750E-01
0.238125E-02   0.238125E-02   0.500000E-02   0.500000E-02
0.000000E+00   0.000000E+00   0.000000E+00   0.000000E+00
0.285750E-01   0.333375E-01   0.333375E-01   0.285750E-01
0.238125E-02   0.238125E-02   0.500000E-02   0.500000E-02
2.540000E-02   2.540000E-02   2.540000E-02   2.540000E-02
```

59

```
                  ELEMENT    15   [   1O]     GROUP       0
0.333375E-01   0.381000E-01   0.381000E-01   0.333375E-01
0.000000E+00   0.000000E+00   0.238125E-02   0.238125E-02
0.000000E+00   0.000000E+00   0.000000E+00   0.000000E+00
0.333375E-01   0.381000E-01   0.381000E-01   0.333375E-01
0.000000E+00   0.000000E+00   0.238125E-02   0.238125E-02
2.540000E-02   2.540000E-02   2.540000E-02   2.540000E-02
                  ELEMENT    16   [   1P]     GROUP       0
0.333375E-01   0.381000E-01   0.381000E-01   0.333375E-01
0.238125E-02   0.238125E-02   0.500000E-02   0.500000E-02
0.000000E+00   0.000000E+00   0.000000E+00   0.000000E+00
0.333375E-01   0.381000E-01   0.381000E-01   0.333375E-01
0.238125E-02   0.238125E-02   0.500000E-02   0.500000E-02
2.540000E-02   2.540000E-02   2.540000E-02   2.540000E-02
                  ELEMENT    17   [   1Q]     GROUP       0
0.381000E-01   0.428625E-01   0.428625E-01   0.381000E-01
0.000000E+00   0.000000E+00   0.238125E-02   0.238125E-02
0.000000E+00   0.000000E+00   0.000000E+00   0.000000E+00
0.381000E-01   0.428625E-01   0.428625E-01   0.381000E-01
0.000000E+00   0.000000E+00   0.238125E-02   0.238125E-02
2.540000E-02   2.540000E-02   2.540000E-02   2.540000E-02
                  ELEMENT    18   [   1R]     GROUP       0
0.381000E-01   0.428625E-01   0.428625E-01   0.381000E-01
0.238125E-02   0.238125E-02   0.500000E-02   0.500000E-02
0.000000E+00   0.000000E+00   0.000000E+00   0.000000E+00
0.381000E-01   0.428625E-01   0.428625E-01   0.381000E-01
0.238125E-02   0.238125E-02   0.500000E-02   0.500000E-02
2.540000E-02   2.540000E-02   2.540000E-02   2.540000E-02
                  ELEMENT    19   [   1S]     GROUP       0
0.428625E-01   0.476250E-01   0.476250E-01   0.428625E-01
0.000000E+00   0.000000E+00   0.238125E-02   0.238125E-02
0.000000E+00   0.000000E+00   0.000000E+00   0.000000E+00
0.428625E-01   0.476250E-01   0.476250E-01   0.428625E-01
0.000000E+00   0.000000E+00   0.238125E-02   0.238125E-02
2.540000E-02   2.540000E-02   2.540000E-02   2.540000E-02
                  ELEMENT    20   [   1T]     GROUP       0
0.428625E-01   0.476250E-01   0.476250E-01   0.428625E-01
0.238125E-02   0.238125E-02   0.500000E-02   0.500000E-02
0.000000E+00   0.000000E+00   0.000000E+00   0.000000E+00
0.428625E-01   0.476250E-01   0.476250E-01   0.428625E-01
0.238125E-02   0.238125E-02   0.500000E-02   0.500000E-02
2.540000E-02   2.540000E-02   2.540000E-02   2.540000E-02
                  ELEMENT    21   [   1U]     GROUP       0
0.000000E+00   0.476250E-02   0.476250E-02   0.000000E+00
0.500000E-02   0.500000E-02   0.100000E-01   0.100000E-01
0.000000E+00   0.000000E+00   0.000000E+00   0.000000E+00
0.000000E+00   0.476250E-02   0.476250E-02   0.000000E+00
0.500000E-02   0.500000E-02   0.100000E-01   0.100000E-01
2.540000E-02   2.540000E-02   2.540000E-02   2.540000E-02
                  ELEMENT    22   [   1V]     GROUP       0
0.238125E-01   0.285750E-01   0.285750E-01   0.238125E-01
0.500000E-02   0.500000E-02   0.100000E-01   0.100000E-01
0.000000E+00   0.000000E+00   0.000000E+00   0.000000E+00
0.238125E-01   0.285750E-01   0.285750E-01   0.238125E-01
0.500000E-02   0.500000E-02   0.100000E-01   0.100000E-01
2.540000E-02   2.540000E-02   2.540000E-02   2.540000E-02
                  ELEMENT    23   [   1W]     GROUP       0
0.476250E-02   0.952500E-02   0.952500E-02   0.476250E-02
0.500000E-02   0.500000E-02   0.100000E-01   0.100000E-01
```

```
0.000000E+00   0.000000E+00   0.000000E+00   0.000000E+00
0.476250E-02   0.952500E-02   0.952500E-02   0.476250E-02
0.500000E-02   0.500000E-02   0.100000E-01   0.100000E-01
2.540000E-02   2.540000E-02   2.540000E-02   2.540000E-02
          ELEMENT   24   [   1X]     GROUP      0
0.952500E-02   0.142875E-01   0.142875E-01   0.952500E-02
0.500000E-02   0.500000E-02   0.100000E-01   0.100000E-01
0.000000E+00   0.000000E+00   0.000000E+00   0.000000E+00
0.952500E-02   0.142875E-01   0.142875E-01   0.952500E-02
0.500000E-02   0.500000E-02   0.100000E-01   0.100000E-01
2.540000E-02   2.540000E-02   2.540000E-02   2.540000E-02
          ELEMENT   25   [   1Y]     GROUP      0
0.142875E-01   0.190500E-01   0.190500E-01   0.142875E-01
0.500000E-02   0.500000E-02   0.100000E-01   0.100000E-01
0.000000E+00   0.000000E+00   0.000000E+00   0.000000E+00
0.142875E-01   0.190500E-01   0.190500E-01   0.142875E-01
0.500000E-02   0.500000E-02   0.100000E-01   0.100000E-01
2.540000E-02   2.540000E-02   2.540000E-02   2.540000E-02
          ELEMENT   26   [   1Z]     GROUP      0
0.190500E-01   0.238125E-01   0.238125E-01   0.190500E-01
0.500000E-02   0.500000E-02   0.100000E-01   0.100000E-01
0.000000E+00   0.000000E+00   0.000000E+00   0.000000E+00
0.190500E-01   0.238125E-01   0.238125E-01   0.190500E-01
0.500000E-02   0.500000E-02   0.100000E-01   0.100000E-01
2.540000E-02   2.540000E-02   2.540000E-02   2.540000E-02
          ELEMENT   27   [   1[]     GROUP      0
0.285750E-01   0.333375E-01   0.333375E-01   0.285750E-01
0.500000E-02   0.500000E-02   0.100000E-01   0.100000E-01
0.000000E+00   0.000000E+00   0.000000E+00   0.000000E+00
0.285750E-01   0.333375E-01   0.333375E-01   0.285750E-01
0.500000E-02   0.500000E-02   0.100000E-01   0.100000E-01
2.540000E-02   2.540000E-02   2.540000E-02   2.540000E-02
          ELEMENT   28   [   1\]     GROUP      0
0.333375E-01   0.381000E-01   0.381000E-01   0.333375E-01
0.500000E-02   0.500000E-02   0.100000E-01   0.100000E-01
0.000000E+00   0.000000E+00   0.000000E+00   0.000000E+00
0.333375E-01   0.381000E-01   0.381000E-01   0.333375E-01
0.500000E-02   0.500000E-02   0.100000E-01   0.100000E-01
2.540000E-02   2.540000E-02   2.540000E-02   2.540000E-02
          ELEMENT   29   [   1]]     GROUP      0
0.381000E-01   0.428625E-01   0.428625E-01   0.381000E-01
0.500000E-02   0.500000E-02   0.100000E-01   0.100000E-01
0.000000E+00   0.000000E+00   0.000000E+00   0.000000E+00
0.381000E-01   0.428625E-01   0.428625E-01   0.381000E-01
0.500000E-02   0.500000E-02   0.100000E-01   0.100000E-01
2.540000E-02   2.540000E-02   2.540000E-02   2.540000E-02
          ELEMENT   30   [   1^]     GROUP      0
0.428625E-01   0.476250E-01   0.476250E-01   0.428625E-01
0.500000E-02   0.500000E-02   0.100000E-01   0.100000E-01
0.000000E+00   0.000000E+00   0.000000E+00   0.000000E+00
0.428625E-01   0.476250E-01   0.476250E-01   0.428625E-01
0.500000E-02   0.500000E-02   0.100000E-01   0.100000E-01
2.540000E-02   2.540000E-02   2.540000E-02   2.540000E-02
          ELEMENT   31   [   1_]     GROUP      0
0.000000E+00   0.476250E-02   0.476250E-02   0.000000E+00
0.100000E-01   0.100000E-01   0.762000E-01   0.762000E-01
0.000000E+00   0.000000E+00   0.000000E+00   0.000000E+00
0.000000E+00   0.476250E-02   0.476250E-02   0.000000E+00
0.100000E-01   0.100000E-01   0.762000E-01   0.762000E-01
```

```
2.540000E-02  2.540000E-02  2.540000E-02  2.540000E-02
         ELEMENT   32   [  1']    GROUP    0
0.238125E-01  0.285750E-01  0.285750E-01  0.238125E-01
0.100000E-01  0.100000E-01  0.762000E-01  0.762000E-01
0.000000E+00  0.000000E+00  0.000000E+00  0.000000E+00
0.238125E-01  0.285750E-01  0.285750E-01  0.238125E-01
0.100000E-01  0.100000E-01  0.762000E-01  0.762000E-01
2.540000E-02  2.540000E-02  2.540000E-02  2.540000E-02
         ELEMENT   33   [  1a]    GROUP    0
0.476250E-02  0.952500E-02  0.952500E-02  0.476250E-02
0.100000E-01  0.100000E-01  0.762000E-01  0.762000E-01
0.000000E+00  0.000000E+00  0.000000E+00  0.000000E+00
0.476250E-02  0.952500E-02  0.952500E-02  0.476250E-02
0.100000E-01  0.100000E-01  0.762000E-01  0.762000E-01
2.540000E-02  2.540000E-02  2.540000E-02  2.540000E-02
         ELEMENT   34   [  1b]    GROUP    0
0.952500E-02  0.142875E-01  0.142875E-01  0.952500E-02
0.100000E-01  0.100000E-01  0.762000E-01  0.762000E-01
0.000000E+00  0.000000E+00  0.000000E+00  0.000000E+00
0.952500E-02  0.142875E-01  0.142875E-01  0.952500E-02
0.100000E-01  0.100000E-01  0.762000E-01  0.762000E-01
2.540000E-02  2.540000E-02  2.540000E-02  2.540000E-02
         ELEMENT   35   [  1c]    GROUP    0
0.142875E-01  0.190500E-01  0.190500E-01  0.142875E-01
0.100000E-01  0.100000E-01  0.762000E-01  0.762000E-01
0.000000E+00  0.000000E+00  0.000000E+00  0.000000E+00
0.142875E-01  0.190500E-01  0.190500E-01  0.142875E-01
0.100000E-01  0.100000E-01  0.762000E-01  0.762000E-01
2.540000E-02  2.540000E-02  2.540000E-02  2.540000E-02
         ELEMENT   36   [  1d]    GROUP    0
0.190500E-01  0.238125E-01  0.238125E-01  0.190500E-01
0.100000E-01  0.100000E-01  0.762000E-01  0.762000E-01
0.000000E+00  0.000000E+00  0.000000E+00  0.000000E+00
0.190500E-01  0.238125E-01  0.238125E-01  0.190500E-01
0.100000E-01  0.100000E-01  0.762000E-01  0.762000E-01
2.540000E-02  2.540000E-02  2.540000E-02  2.540000E-02
         ELEMENT   37   [  1e]    GROUP    0
0.285750E-01  0.333375E-01  0.333375E-01  0.285750E-01
0.100000E-01  0.100000E-01  0.762000E-01  0.762000E-01
0.000000E+00  0.000000E+00  0.000000E+00  0.000000E+00
0.285750E-01  0.333375E-01  0.333375E-01  0.285750E-01
0.100000E-01  0.100000E-01  0.762000E-01  0.762000E-01
2.540000E-02  2.540000E-02  2.540000E-02  2.540000E-02
         ELEMENT   38   [  1f]    GROUP    0
0.333375E-01  0.381000E-01  0.381000E-01  0.333375E-01
0.100000E-01  0.100000E-01  0.762000E-01  0.762000E-01
0.000000E+00  0.000000E+00  0.000000E+00  0.000000E+00
0.333375E-01  0.381000E-01  0.381000E-01  0.333375E-01
0.100000E-01  0.100000E-01  0.762000E-01  0.762000E-01
2.540000E-02  2.540000E-02  2.540000E-02  2.540000E-02
         ELEMENT   39   [  1g]    GROUP    0
0.381000E-01  0.428625E-01  0.428625E-01  0.381000E-01
0.100000E-01  0.100000E-01  0.762000E-01  0.762000E-01
0.000000E+00  0.000000E+00  0.000000E+00  0.000000E+00
0.381000E-01  0.428625E-01  0.428625E-01  0.381000E-01
0.100000E-01  0.100000E-01  0.762000E-01  0.762000E-01
2.540000E-02  2.540000E-02  2.540000E-02  2.540000E-02
         ELEMENT   40   [  1h]    GROUP    0
0.428625E-01  0.476250E-01  0.476250E-01  0.428625E-01
```

```
0.100000E-01   0.100000E-01   0.762000E-01   0.762000E-01
0.000000E+00   0.000000E+00   0.000000E+00   0.000000E+00
0.428625E-01   0.476250E-01   0.476250E-01   0.428625E-01
0.100000E-01   0.100000E-01   0.762000E-01   0.762000E-01
2.540000E-02   2.540000E-02   2.540000E-02   2.540000E-02
***** CURVED SIDE DATA *****
0 Curved sides follow IEDGE,IEL,CURVE(I),I=1,5, CCURVE
***** BOUNDARY CONDITIONS *****
***** NO FLUID    BOUNDARY CONDITIONS *****
***** THERMAL BOUNDARY CONDITIONS *****
I 1 1 0.000000E+00 0.000000E+00 0.000000E+00 0.000000E+00 0.000000E+00
E 1 2 5.00000       4.00000       0.000000E+00 0.000000E+00 0.000000E+00
E 1 3 2.00000       1.00000       0.000000E+00 0.000000E+00 0.000000E+00
c 1 4 2.00000       1.00000       0.000000E+00 0.000000E+00 0.000000E+00
          TINF=297.594
          HC=3309.2*(ABS(TEMP-TINF))**(0.25)
c 1 5 2.00000       3.00000       0.000000E+00 0.000000E+00 0.000000E+00
          TINF=297.594
          HC=3309.2*(ABS(TEMP-TINF))**(0.25)
f 1 6 1.00000       5.00000       0.000000E+00 0.000000E+00 0.000000E+00
          FLUX=148760000.0
E 2 1 1.00000       3.00000       0.000000E+00 0.000000E+00 0.000000E+00
E 2 2 6.00000       4.00000       0.000000E+00 0.000000E+00 0.000000E+00
E 2 3 21.0000       1.00000       0.000000E+00 0.000000E+00 0.000000E+00
c 2 4 2.00000       6.00000       0.000000E+00 0.000000E+00 0.000000E+00
          TINF=297.594
          HC=3309.2*(ABS(TEMP-TINF))**(0.25)
c 2 5 2.00000       8.00000       0.000000E+00 0.000000E+00 0.000000E+00
          TINF=297.594
          HC=3309.2*(ABS(TEMP-TINF))**(0.25)
c 2 6 2.00000       10.0000       0.000000E+00 0.000000E+00 0.000000E+00
          TINF=297.594
          HC=3309.2*(ABS(TEMP-TINF))**(0.25)
I 3 1 0.000000E+00 0.000000E+00 0.000000E+00 0.000000E+00 0.000000E+00
E 3 2 13.0000       4.00000       0.000000E+00 0.000000E+00 0.000000E+00
E 3 3 4.00000       1.00000       0.000000E+00 0.000000E+00 0.000000E+00
E 3 4 11.0000       2.00000       0.000000E+00 0.000000E+00 0.000000E+00
c 3 5 2.00000       12.0000       0.000000E+00 0.000000E+00 0.000000E+00
          TINF=297.594
          HC=3309.2*(ABS(TEMP-TINF))**(0.25)
f 3 6 1.00000       14.0000       0.000000E+00 0.000000E+00 0.000000E+00
          FLUX=148760000.0
E 4 1 3.00000       3.00000       0.000000E+00 0.000000E+00 0.000000E+00
E 4 2 14.0000       4.00000       0.000000E+00 0.000000E+00 0.000000E+00
E 4 3 22.0000       1.00000       0.000000E+00 0.000000E+00 0.000000E+00
E 4 4 12.0000       2.00000       0.000000E+00 0.000000E+00 0.000000E+00
c 4 5 2.00000       15.0000       0.000000E+00 0.000000E+00 0.000000E+00
          TINF=297.594
          HC=3309.2*(ABS(TEMP-TINF))**(0.25)
c 4 6 2.00000       17.0000       0.000000E+00 0.000000E+00 0.000000E+00
          TINF=297.594
          HC=3309.2*(ABS(TEMP-TINF))**(0.25)
I 5 1 0.000000E+00 0.000000E+00 0.000000E+00 0.000000E+00 0.000000E+00
E 5 2 7.00000       4.00000       0.000000E+00 0.000000E+00 0.000000E+00
E 5 3 6.00000       1.00000       0.000000E+00 0.000000E+00 0.000000E+00
E 5 4 1.00000       2.00000       0.000000E+00 0.000000E+00 0.000000E+00
c 5 5 2.00000       19.0000       0.000000E+00 0.000000E+00 0.000000E+00
          TINF=297.594
          HC=3309.2*(ABS(TEMP-TINF))**(0.25)
```

```
f 5 6 1.00000        21.0000        0.000000E+00 0.000000E+00 0.000000E+00
        FLUX=148760000.0
E 6 1 5.00000        3.00000        0.000000E+00 0.000000E+00 0.000000E+00
E 6 2 8.00000        4.00000        0.000000E+00 0.000000E+00 0.000000E+00
E 6 3 23.0000        1.00000        0.000000E+00 0.000000E+00 0.000000E+00
E 6 4 2.00000        2.00000        0.000000E+00 0.000000E+00 0.000000E+00
c 6 5 2.00000        22.0000        0.000000E+00 0.000000E+00 0.000000E+00
        TINF=297.594
        HC=3309.2*(ABS(TEMP-TINF))**(0.25)
c 6 6 2.00000        24.0000        0.000000E+00 0.000000E+00 0.000000E+00
        TINF=297.594
        HC=3309.2*(ABS(TEMP-TINF))**(0.25)
I 7 1 0.000000E+00 0.000000E+00 0.000000E+00 0.000000E+00 0.000000E+00
E 7 2 9.00000        4.00000        0.000000E+00 0.000000E+00 0.000000E+00
E 7 3 8.00000        1.00000        0.000000E+00 0.000000E+00 0.000000E+00
E 7 4 5.00000        2.00000        0.000000E+00 0.000000E+00 0.000000E+00
c 7 5 2.00000        26.0000        0.000000E+00 0.000000E+00 0.000000E+00
        TINF=297.594
        HC=3309.2*(ABS(TEMP-TINF))**(0.25)
f 7 6 1.00000        28.0000        0.000000E+00 0.000000E+00 0.000000E+00
        FLUX=37190000.0
E 8 1 7.00000        3.00000        0.000000E+00 0.000000E+00 0.000000E+00
E 8 2 10.0000        4.00000        0.000000E+00 0.000000E+00 0.000000E+00
E 8 3 24.0000        1.00000        0.000000E+00 0.000000E+00 0.000000E+00
E 8 4 6.00000        2.00000        0.000000E+00 0.000000E+00 0.000000E+00
c 8 5 2.00000        29.0000        0.000000E+00 0.000000E+00 0.000000E+00
        TINF=297.594
        HC=3309.2*(ABS(TEMP-TINF))**(0.25)
c 8 6 2.00000        31.0000        0.000000E+00 0.000000E+00 0.000000E+00
        TINF=297.594
        HC=3309.2*(ABS(TEMP-TINF))**(0.25)
I 9 1 0.000000E+00 0.000000E+00 0.000000E+00 0.000000E+00 0.000000E+00
E 9 2 11.0000        4.00000        0.000000E+00 0.000000E+00 0.000000E+00
E 9 3 10.0000        1.00000        0.000000E+00 0.000000E+00 0.000000E+00
E 9 4 7.00000        2.00000        0.000000E+00 0.000000E+00 0.000000E+00
c 9 5 2.00000        33.0000        0.000000E+00 0.000000E+00 0.000000E+00
        TINF=297.594
        HC=3309.2*(ABS(TEMP-TINF))**(0.25)
f 9 6 1.00000        35.0000        0.000000E+00 0.000000E+00 0.000000E+00
    FLUX=37190000.0
E 10 1 9.00000        3.00000        0.000000E+00 0.000000E+00 0.000000E+00
E 10 2 12.0000        4.00000        0.000000E+00 0.000000E+00 0.000000E+00
E 10 3 25.0000        1.00000        0.000000E+00 0.000000E+00 0.000000E+00
E 10 4 8.00000        2.00000        0.000000E+00 0.000000E+00 0.000000E+00
c 10 5 2.00000        36.0000        0.000000E+00 0.000000E+00 0.000000E+00
        TINF=297.594
        HC=3309.2*(ABS(TEMP-TINF))**(0.25)
c 10 6 2.00000        38.0000        0.000000E+00 0.000000E+00 0.000000E+00
        TINF=297.594
        HC=3309.2*(ABS(TEMP-TINF))**(0.25)
I 11 1 0.000000E+00 0.000000E+00 0.000000E+00 0.000000E+00 0.000000E+00
E 11 2 3.00000        4.00000        0.000000E+00 0.000000E+00 0.000000E+00
E 11 3 12.0000        1.00000        0.000000E+00 0.000000E+00 0.000000E+00
E 11 4 9.00000        2.00000        0.000000E+00 0.000000E+00 0.000000E+00
c 11 5 2.00000        40.0000        0.000000E+00 0.000000E+00 0.000000E+00
        TINF=297.594
        HC=3309.2*(ABS(TEMP-TINF))**(0.25)
f 11 6 1.00000        42.0000        0.000000E+00 0.000000E+00 0.000000E+00
        FLUX=148760000.0
```

```
E 12 1   11.0000       3.00000        0.000000E+00 0.000000E+00 0.000000E+00
E 12 2   4.00000       4.00000        0.000000E+00 0.000000E+00 0.000000E+00
E 12 3   26.0000       1.00000        0.000000E+00 0.000000E+00 0.000000E+00
E 12 4   10.0000       2.00000        0.000000E+00 0.000000E+00 0.000000E+00
c 12 5   2.00000       43.0000        0.000000E+00 0.000000E+00 0.000000E+00
         TINF=297.594
         HC=3309.2*(ABS(TEMP-TINF))**(0.25)
c 12 6   2.00000       45.0000        0.000000E+00 0.000000E+00 0.000000E+00
         TINF=297.594
         HC=3309.2*(ABS(TEMP-TINF))**(0.25)
I 13 1 0.000000E+00 0.000000E+00 0.000000E+00 0.000000E+00 0.000000E+00
E 13 2 15.0000        4.00000        0.000000E+00 0.000000E+00 0.000000E+00
E 13 3 14.0000        1.00000        0.000000E+00 0.000000E+00 0.000000E+00
E 13 4 3.00000        2.00000        0.000000E+00 0.000000E+00 0.000000E+00
c 13 5 2.00000        47.0000        0.000000E+00 0.000000E+00 0.000000E+00
         TINF=297.594
         HC=3309.2*(ABS(TEMP-TINF))**(0.25)
f 13 6 1.00000        49.0000        0.000000E+00 0.000000E+00 0.000000E+00
         FLUX=148760000.0
E 14 1 13.0000        3.00000        0.000000E+00 0.000000E+00 0.000000E+00
E 14 2 16.0000        4.00000        0.000000E+00 0.000000E+00 0.000000E+00
E 14 3 27.0000        1.00000        0.000000E+00 0.000000E+00 0.000000E+00
E 14 4 4.00000        2.00000        0.000000E+00 0.000000E+00 0.000000E+00
c 14 5 2.00000        50.0000        0.000000E+00 0.000000E+00 0.000000E+00
         TINF=297.594
         HC=3309.2*(ABS(TEMP-TINF))**(0.25)
c 14 6 2.00000        52.0000        0.000000E+00 0.000000E+00 0.000000E+00
         TINF=297.594
         HC=3309.2*(ABS(TEMP-TINF))**(0.25)
I 15 1 0.000000E+00 0.000000E+00 0.000000E+00 0.000000E+00 0.000000E+00
E 15 2 17.0000        4.00000        0.000000E+00 0.000000E+00 0.000000E+00
E 15 3 16.0000        1.00000        0.000000E+00 0.000000E+00 0.000000E+00
E 15 4 13.0000        2.00000        0.000000E+00 0.000000E+00 0.000000E+00
c 15 5 2.00000        54.0000        0.000000E+00 0.000000E+00 0.000000E+00
         TINF=297.594
         HC=3309.2*(ABS(TEMP-TINF))**(0.25)
f 15 6 1.00000        56.0000        0.000000E+00 0.000000E+00 0.000000E+00
         FLUX=148760000.0
E 16 1 15.0000        3.00000        0.000000E+00 0.000000E+00 0.000000E+00
E 16 2 18.0000        4.00000        0.000000E+00 0.000000E+00 0.000000E+00
E 16 3 28.0000        1.00000        0.000000E+00 0.000000E+00 0.000000E+00
E 16 4 14.0000        2.00000        0.000000E+00 0.000000E+00 0.000000E+00
c 16 5 2.00000        57.0000        0.000000E+00 0.000000E+00 0.000000E+00
         TINF=297.594
         HC=3309.2*(ABS(TEMP-TINF))**(0.25)
c 16 6 2.00000        59.0000        0.000000E+00 0.000000E+00 0.000000E+00
         TINF=297.594
         HC=3309.2*(ABS(TEMP-TINF))**(0.25)
I 17 1 0.000000E+00 0.000000E+00 0.000000E+00 0.000000E+00 0.000000E+00
E 17 2 19.0000        4.00000        0.000000E+00 0.000000E+00 0.000000E+00
E 17 3 18.0000        1.00000        0.000000E+00 0.000000E+00 0.000000E+00
E 17 4 15.0000        2.00000        0.000000E+00 0.000000E+00 0.000000E+00
c 17 5 2.00000        61.0000        0.000000E+00 0.000000E+00 0.000000E+00
         TINF=297.594
         HC=3309.2*(ABS(TEMP-TINF))**(0.25)
f 17 6 1.00000        63.0000        0.000000E+00 0.000000E+00 0.000000E+00
         FLUX=148760000.0
E 18 1 17.0000        3.00000        0.000000E+00 0.000000E+00 0.000000E+00
E 18 2 20.0000        4.00000        0.000000E+00 0.000000E+00 0.000000E+00
```

```
E  18  3  29.0000       1.00000        0.000000E+00  0.000000E+00  0.000000E+00
E  18  4  16.0000       2.00000        0.000000E+00  0.000000E+00  0.000000E+00
c  18  5  2.00000       64.0000        0.000000E+00  0.000000E+00  0.000000E+00
          TINF=297.594
          HC=3309.2*(ABS(TEMP-TINF))**(0.25)
c  18  6  2.00000       66.0000        0.000000E+00  0.000000E+00  0.000000E+00
          TINF=297.594
          HC=3309.2*(ABS(TEMP-TINF))**(0.25)
I  19  1  0.000000E+00  0.000000E+00   0.000000E+00  0.000000E+00  0.000000E+00
c  19  2  2.00000       68.0000        0.000000E+00  0.000000E+00  0.000000E+00
          TINF=297.597
          HC=3309.2*(ABS(TEMP-TINF))**(0.25)
E  19  3  20.0000       1.00000        0.000000E+00  0.000000E+00  0.000000E+00
E  19  4  17.0000       2.00000        0.000000E+00  0.000000E+00  0.000000E+00
c  19  5  2.00000       70.0000        0.000000E+00  0.000000E+00  0.000000E+00
          TINF=297.594
          HC=3309.2*(ABS(TEMP-TINF))**(0.25)
f  19  6  1.00000       72.0000        0.000000E+00  0.000000E+00  0.000000E+00
          FLUX=148760000.0
E  20  1  19.0000       3.00000        0.000000E+00  0.000000E+00  0.000000E+00
c  20  2  2.00000       73.0000        0.000000E+00  0.000000E+00  0.000000E+00
          TINF=297.594
          HC=3309.2*(ABS(TEMP-TINF))**(0.25)
E  20  3  30.0000       1.00000        0.000000E+00  0.000000E+00  0.000000E+00
E  20  4  18.0000       2.00000        0.000000E+00  0.000000E+00  0.000000E+C0
c  20  5  2.00000       75.0000        0.000000E+00  0.000000E+00  0.000000E+00
          TINF=297.594
          HC=3309.2*(ABS(TEMP-TINF))**(0.25)
c  20  6  2.00000       77.0000        0.000000E+00  0.000000E+00  0.000000E+00
          TINF=297.594
          HC=3309.2*(ABS(TEMP-TINF))**(0.25)
E  21  1  2.00000       3.00000        0.000000E+00  0.000000E+00  0.000000E+00
E  21  2  23.0000       4.00000        0.000000E+00  0.000000E+00  0.000000E+00
E  21  3  31.0000       1.00000        0.000000E+00  0.000000E+00  0.000000E+00
c  21  4  2.00000       81.0000        0.000000E+00  0.000000E+00  0 000000E+00
          TINF=297.594
          HC=3309.2*(ABS(TEMP-TINF))**(0.25)
c  21  5  2.00000       83.0000        0.000000E+00  0.000000E+00  0.000000E+00
          TINF=297.594
          HC=3309.2*(ABS(TEMP-TINF))**(0.25)
c  21  6  2.00000       85.0000        0.000000E+00  0.000000E+00  0.000000E+00
          TINF=297.594
          HC=3309.2*(ABS(TEMP-TINF))**(0.25)
E  22  1  4.00000       3.00000        0.000000E+00  0.000000E+00  0.000000E+00
E  22  2  27.0000       4.00000        0.000000E+00  0.000000E+00  0.000000E+00
E  22  3  32.0000       1.00000        0.000000E+00  0.000000E+00  0.000000E+00
E  22  4  26.0000       2.00000        0.000000E+00  0.000000E+00  0.000000E+00
c  22  5  2.00000       89.0000        0.000000E+00  0.000000E+00  0.000000E+00
          TINF=297.594
          HC=3309.2*(ABS(TEMP-TINF))**(0.25)
c  22  6  2.00000       91.0000        0.000000E+00  0.000000E+00  0.000000E+00
          TINF=297.594
          HC=3309.2*(ABS(TEMP-TINF))**(0.25)
E  23  1  6.00000       3.00000        0.000000E+00  0.000000E+00  0.000000E+00
E  23  2  24.0000       4.00000        0.000000E+00  0.000000E+00  0.000000E+00
E  23  3  33.0000       1.00000        0.000000E+00  0.000000E+00  0.000000E+00
E  23  4  21.0000       2.00000        0.000000E+00  0.000000E+00  0.000000E+00
c  23  5  2.00000       95.0000        0.000000E+00  0.000000E+00  0.000000E+00
          TINF=297.594
```

```
            HC=3309.2*(ABS(TEMP-TINF))**(0.25)
c 23 6   2.00000        97.0000       0.000000E+00 0.000000E+00 0.000000E+00
            TINF=297.594
            HC=3309.2*(ABS(TEMP-TINF))**(0.25)
E 24 1   8.00000        3.00000       0.000000E+00 0.000000E+00 0.000000E+00
E 24 2   25.0000        4.00000       0.000000E+00 0.000000E+00 0.000000E+00
E 24 3   34.0000        1.00000       0.000000E+00 0.000000E+00 0.000000E+00
E 24 4   23.0000        2.00000       0.000000E+00 0.000000E+00 0.000000E+00
c 24 5   2.00000        101.000       0.000000E+00 0.000000E+00 0.000000E+00
            TINF=297.594
            HC=3309.2*(ABS(TEMP-TINF))**(0.25)
c 24 6   2.00000        103.000       0.000000E+00 0.000000E+00 0.000000E+00
            TINF=297.594
            HC=3309.2*(ABS(TEMP-TINF))**(0.25)
E 25 1   10.0000        3.00000       0.000000E+00 0.000000E+00 0.000000E+00
E 25 2   26.0000        4.00000       0.000000E+00 0.000000E+00 0.000000E+00
E 25 3   35.0000        1.00000       0.000000E+00 0.000000E+00 0.000000E+00
E 25 4   24.0000        2.00000       0.000000E+00 0.000000E+00 0.000000E+00
c 25 5   2.00000        107.000       0.000000E+00 0.000000E+00 0.000000E+00
            TINF=297.594
            HC=3309.2*(ABS(TEMP-TINF))**(0.25)
c 25 6   2.00000        109.000       0.000000E+00 0.000000E+00 0.000000E+00
            TINF=297.594
            HC=3309.2*(ABS(TEMP-TINF))**(0.25)
E 26 1   12.0000        3.00000       0.000000E+00 0.000000E+00 0.000000E+00
E 26 2   22.0000        4.00000       0.000000E+00 0.000000E+00 0.000000E+00
E 26 3   36.0000        1.00000       0.000000E+00 0.000000E+00 0.000000E+00
E 26 4   25.0000        2.00000       0.000000E+00 0.000000E+00 0.000000E+00
c 26 5   2.00000        113.000       0.000000E+00 0.000000E+00 0.000000E+00
            TINF=297.594
            HC=3309.2*(ABS(TEMP-TINF))**(0.25)
c 26 6   2.00000        115.000       0.000000E+00 0.000000E+00 0.000000E+00
            TINF=297.594
            HC=3309.2*(ABS(TEMP-TINF))**(0.25)
E 27 1   14.0000        3.00000       0.000000E+00 0.000000E+00 0.000000E+00
E 27 2   28.0000        4.00000       0.000000E+00 0.000000E+00 0.000000E+00
E 27 3   37.0000        1.00000       0.000000E+00 0.000000E+00 0.000000E+00
E 27 4   22.0000        2.00000       0.000000E+00 0.000000E+00 0.000000E+00
c 27 5   2.00000        119.000       0.000000E+00 0.000000E+00 0.000000E+00
            TINF=297.594
            HC=3309.2*(ABS(TEMP-TINF))**(0.25)
c 27 6   2.00000        121.000       0.000000E+00 0.000000E+00 0.000000E+00
            TINF=297.594
            HC=3309.2*(ABS(TEMP-TINF))**(0.25)
E 28 1   16.0000        3.00000       0.000000E+00 0.000000E+00 0.000000E+00
E 28 2   29.0000        4.00000       0.000000E+00 0.000000E+00 0.000000E+00
E 28 3   38.0000        1.00000       0.000000E+00 0.000000E+00 0.000000E+00
E 28 4   27.0000        2.00000       0.000000E+00 0.000000E+00 0.000000E+00
c 28 5   2.00000        125.000       0.000000E+00 0.000000E+00 0.000000E+00
            TINF=297.594
            HC=3309.2*(ABS(TEMP-TINF))**(0.25)
c 28 6   2.00000        127.000       0.000000E+00 0.000000E+00 0.000000E+00
            TINF=297.594
            HC=3309.2*(ABS(TEMP-TINF))**(0.25)
E 29 1   18.0000        3.00000       0.000000E+00 0.000000E+00 0.000000E+00
E 29 2   30.0000        4.00000       0.000000E+00 0.000000E+00 0.000000E+00
E 29 3   39.0000        1.00000       0.000000E+00 0.000000E+00 0.000000E+00
E 29 4   28.0000        2.00000       0.000000E+00 0.000000E+00 0.000000E+00
c 29 5   2.00000        131.000       0.000000E+00 0.000000E+00 0.000000E+00
```

```
          TINF=297.594
          HC=3309.2*(ABS(TEMP-TINF))**(0.25)
c 29 6    2.00000          133.000      0.000000E+00 0.000000E+00 0.000000E+00
          TINF=297.594
          HC=3309.2*(ABS(TEMP-TINF))**(0.25)
E 30 1    20.0000          3.00000      0.000000E+00 0.000000E+00 0.000000E+00
c 30 2    2.00000          135.000      0.000000E+00 0.000000E+00 0.000000E+00
          TINF=297.594
          HC=3309.2*(ABS(TEMP-TINF))**(0.25)
E 30 3    40.0000          1.00000      0.000000E+00 0.000000E+00 0.000000E+00
E 30 4    29.0000          2.00000      0.000000E+00 0.000000E+00 0.000000E+00
c 30 5    2.00000          139.000      0.000000E+00 0.000000E+00 0.000000E+00
          TINF=297.594
          HC=3309.2*(ABS(TEMP-TINF))**(0.25)
c 30 6    2.00000          141.000      0.000000E+00 0.000000E+00 0.000000E+00
          TINF=297.594
          HC=3309.2*(ABS(TEMP-TINF))**(0.25)
E 31 1    21.0000          3.00000      0.000000E+00 0.000000E+00 0.000000E+00
E 31 2    33.0000          4.00000      0.000000E+00 0.000000E+00 0.000000E+00
c 31 3    2.00000          79.0000      0.000000E+00 0.000000E+00 0.000000E+00
          TINF=297.594
          HC=3309.2*(ABS(TEMP-TINF))**(0.25)
c 31 4    2.00000          81.0000      0.000000E+00 0.000000E+00 0.000000E+00
          TINF=297.594
          HC=3309.2*(ABS(TEMP-TINF))**(0.25)
c 31 5    2.00000          83.0000      0.000000E+00 0.000000E+00 0.000000E+00
          TINF=297.594
          HC=3309.2*(ABS(TEMP-TINF))**(0.25)
c 31 6    2.00000          85.0000      0.000000E+00 0.000000E+00 0.000000E+00
          TINF=297.594
          HC=3309.2*(ABS(TEMP-TINF))**(0.25)
E 32 1    22.0000          3.00000      0.000000E+00 0.000000E+00 0.000000E+00
E 32 2    37.0000          4.00000      0.000000E+00 0.000000E+00 0.000000E+00
c 32 3    2.00000          87.0000      0.000000E+00 0.000000E+00 0.000000E+00
          TINF=297.594
          HC=3309.2*(ABS(TEMP-TINF))**(0.25)
E 32 4    36.0000          2.00000      0.000000E+00 0.000000E+00 0.000000E+00
c 32 5    2.00000          89.0000      0.000000E+00 0.000000E+00 0.000000E+00
          TINF=297.594
          HC=3309.2*(ABS(TEMP-TINF))**(0.25)
c 32 6    2.00000          91.0000      0.000000E+00 0.000000E+00 0.000000E+00
          TINF=297.594
          HC=3309.2*(ABS(TEMP-TINF))**(0.25)
E 33 1    23.0000          3.00000      0.000000E+00 0.000000E+00 0.000000E+00
E 33 2    34.0000          4.00000      0.000000E+00 0.000000E+00 0.000000E+00
c 33 3    2.00000          93.0000      0.000000E+00 0.000000E+00 0.000000E+00
          TINF=297.594
          HC=3309.2*(ABS(TEMP-TINF))**(0.25)
E 33 4    31.0000          2.00000      0.000000E+00 0.000000E+00 0.000000E+00
c 33 5    2.00000          95.0000      0.000000E+00 0.000000E+00 0.000000E+00
          TINF=297.594
          HC=3309.2*(ABS(TEMP-TINF))**(0.25)
c 33 6    2.00000          97.0000      0.000000E+00 0.000000E+00 0.000000E+00
          TINF=297.594
          HC=3309.2*(ABS(TEMP-TINF))**(0.25)
E 34 1    24.0000          3.00000      0.000000E+00 0.000000E+00 0.000000E+00
E 34 2    35.0000          4.00000      0.000000E+00 0.000000E+00 0.000000E+00
c 34 3    2.00000          99.0000      0.000000E+00 0.000000E+00 0.000000E+00
          TINF=297.594
```

```
                HC=3309.2*(ABS(TEMP-TINF))**(0.25)
E  34  4    33.0000           2.00000      0.000000E+00  0.000000E+00  0.000000E+00
c  34  5    2.00000           101.000      0.000000E+00  0.000000E+00  0.000000E+00
                TINF=297.594
                HC=3309.2*(ABS(TEMP-TINF))**(0.25)
c  34  6    2.00000           103.000      0.000000E+00  0.000000E+00  0.000000E+00
                TINF=297.594
                HC=3309.2*(ABS(TEMP-TINF))**(0.25)
E  35  1    25.0000           3.00000      0.000000E+00  0.000000E+00  0.000000E+00
E  35  2    36.0000           4.00000      0.000000E+00  0.000000E+00  0.000000E+00
c  35  3    2.00000           105.000      0.000000E+00  0.000000E+00  0.000000E+00
                TINF=297.594
                HC=3309.2*(ABS(TEMP-TINF))**(0.25)
E  35  4    34.0000           2.00000      0.000000E+00  0.000000E+00  0.000000E+00
c  35  5    2.00000           107.000      0.000000E+00  0.000000E+00  0.000000E+00
                TINF=297.594
                HC=3309.2*(ABS(TEMP-TINF))**(0.25)
c  35  6    2.00000           109.000      0.000000E+00  0.000000E+00  0.000000E+00
                TINF=297.594
                HC=3309.2*(ABS(TEMP-TINF))**(0.25)
E  36  1    26.0000           3.00000      0.000000E+00  0.000000E+00  0.000000E+00
E  36  2    32.0000           4.00000      0.000000E+00  0.000000E+00  0.000000E+00
c  36  3    2.00000           111.000      0.000000E+00  0.000000E+00  0.000000E+00
                TINF=297.594
                HC=3309.2*(ABS(TEMP-TINF))**(0.25)
E  36  4    35.0000           2.00000      0.000000E+00  0.000000E+00  0.000000E+00
c  36  5    2.00000           113.000      0.000000E+00  0.000000E+00  0.000000E+00
                TINF=297.594
                HC=3309.2*(ABS(TEMP-TINF))**(0.25)
c  36  6    2.00000           115.000      0.000000E+00  0.000000E+00  0.000000E+00
                TINF=297.594
                HC=3309.2*(ABS(TEMP-TINF))**(0.25)
E  37  1    27.0000           3.00000      0.000000E+00  0.000000E+00  0.000000E+00
E  37  2    38.0000           4.00000      0.000000E+00  0.000000E+00  0.000000E+00
c  37  3    2.00000           117.000      0.000000E+00  0.000000E+00  0.000000E+00
                TINF=297.594
                HC=3309.2*(ABS(TEMP-TINF))**(0.25)
E  37  4    32.0000           2.00000      0.000000E+00  0.000000E+00  0.000000E+00
c  37  5    2.00000           119.000      0.000000E+00  0.000000E+00  0.000000E+00
                TINF=297.594
                HC=3309.2*(ABS(TEMP-TINF))**(0.25)
c  37  6    2.00000           121.000      0.000000E+00  0.000000E+00  0.000000E+00
                TINF=297.594
                HC=3309.2*(ABS(TEMP-TINF))**(0.25)
E  38  1    28.0000           3.00000      0.000000E+00  0.000000E+00  0.000000E+00
E  38  2    39.0000           4.00000      0.000000E+00  0.000000E+00  0.000000E+00
c  38  3    2.00000           123.000      0.000000E+00  0.000000E+00  0.000000E+00
                TINF=297.594
                HC=3309.2*(ABS(TEMP-TINF))**(0.25)
E  38  4    37.0000           2.00000      0.000000E+00  0.000000E+00  0.000000E+00
c  38  5    2.00000           125.000      0.000000E+00  0.000000E+00  0.000000E+00
                TINF=297.594
                HC=3309.2*(ABS(TEMP-TINF))**(0.25)
c  38  6    2.00000           127.000      0.000000E+00  0.000000E+00  0.000000E+00
                TINF=297.594
                HC=3309.2*(ABS(TEMP-TINF))**(0.25)
E  39  1    29.0000           3.00000      0.000000E+00  0.000000E+00  0.000000E+00
E  39  2    40.0000           4.00000      0.000000E+00  0.000000E+00  0.000000E+00
c  39  3    2.00000           129.000      0.000000E+00  0.000000E+00  0.000000E+00
```

69

```
          TINF=297.594
          HC=3309.2*(ABS(TEMP-TINF))**(0.25)
E 39 4    38.0000       2.00000      0.000000E+00 0.000000E+00 0.000000E+
c 39 5    2.00000       131.000      0.000000E+00 0.000000E+00 0.000000E+
          TINF=297.594
          HC=3309.2*(ABS(TEMP-TINF))**(0.25)
c 39 6    2.00000       133.000      0.000000E+00 0.000000E+00 0.000000E+00
          TINF=297.594
          HC=3309.2*(ABS(TEMP-TINF))**(0.25)
E 40 1    30.0000       3.00000      0.000000E+00 0.000000E+00 0.000000E+00
c 40 2    2.00000       135.000      0.000000E+00 0.000000E+00 0.000000E+00
          TINF=297.594
          HC=3309.2*(ABS(TEMP-TINF))**(0.25)
c 40 3    2.00000       137.000      0.000000E+00 0.000000E+00 0.000000E+00
          TINF=297.594
          HC=3309.2*(ABS(TEMP-TINF))**(0.25)
E 40 4    39.0000       2.00000      0.000000E+00 0.000000E+00 0.000000E+00
c 40 5    2.00000       139.000      0.000000E+00 0.000000E+00 0.000000E+00
          TINF=297.594
          HC=3309.2*(ABS(TEMP-TINF))**(0.25)
c 40 6    2.00000       141.000      0.000000E+00 0.000000E+00 0.000000E+00
          TINF=297.594
          HC=3309.2*(ABS(TEMP-TINF))**(0.25)
          0 PRESOLVE/RESTART OPTIONS   *****
          7            INITIAL CONDITIONS *****


          C Default
          TEMP=297.594
C Default
C Default
***** DRIVE FORCE DATA ***** BODY FORCE, FLOW, Q
          4                   Lines of Drive force data follow
C
C
C
C
 ***** Variable Property Data ***** Overrrides Parameter data.
          1 Lines follow.
          0 PACKETS OF DATA FOLLOW
***** HISTORY AND INTEGRAL DATA *****
     3    POINTS.   Hcode, I,J,H,IEL
XYZ T     H       1    5    5    3
XYZ T     H       1    5    5    4
XYZ T     H       1    5    5    22
***** OUTPUT FIELD SPECIFICATION ****
          6 SPECIFICATIONS FOLLOW
F         COORDINATES
F         VELOCITY
F         PRESSURE
T         TEMPERATURE
F         TEMPERATURE GRADIENT
          0         PASSIVE SCALARS
***** OBJECT SPECIFICATION *****
0 Surface Objects
0 Volume  Objects
0 Edge    Objects
0 Point   Objects
```

APPENDIX B

FORTRAN code used to establish model boundary conditions
(NEKTON user File)

71

```
C******************************************************************
C   USER SPECIFIED SUBROUTINES:
C       - boundary conditions
C       - initial conditions
C       - variable properties
C       - forcing function for fluid (f)
C       - forcing function for passive scalar (q)
C       - general purpose routine for checking errors etc.
C******************************************************************
C
        SUBROUTINE USERVP (IX,IY,IZ,IEL)
        INCLUDE 'SIZE'
C       INCLUDE 'TSTEP'
        INCLUDE 'TOTAL'
        INCLUDE 'NEKUSE'
C
          UDIFF =0.
          UTRANS=0.
          IF(.FALSE.)THEN
        ENDIF
        IF(UDIFF.LE.0.0 .OR.UTRANS.LE.0.0)THEN
                PRINT*,'        **ERROR** '
                PRINT*,'NONPOSITIVE QUANTITY IN USER-SUPPLIED'
                PRINT*,'FORTRAN FUNCTION'
                PRINT*,'IX,IY,IZ,IEL,IFIELD,ISTEP:'
                PRINT*, IX,IY,IZ,IEL,IFIELD,ISTEP
                PRINT*,'UDIFF,UTRANS '
                PRINT*, UDIFF,UTRANS
                STOP
        ENDIF
        RETURN
        END
C
        SUBROUTINE USERF   (IX,IY,IZ,IEL)
        INCLUDE 'SIZE'
        INCLUDE 'TSTEP'
C       INCLUDE 'TOTAL'
        INCLUDE 'NEKUSE'
C
        FFX = 0.0
        FFY = 0.0
        FFZ = 0.0
C
        RETURN
        END
C
        SUBROUTINE USERQ   (IX,IY,IZ,IEL)
        INCLUDE 'SIZE'
        INCLUDE 'TOTAL'
        INCLUDE 'NEKUSE'
C
        QVOL   = 0.0
        SOURCE = 0.0
        RETURN
        END
        SUBROUTINE USERCHK
        INCLUDE 'SIZE'
        INCLUDE 'TOTAL'
        RETURN
```

```
      END
C
      SUBROUTINE USERBC (IX,IY,IZ,ISIDE,IEL)
      INCLUDE 'SIZE'
      INCLUDE 'TSTEP'
C     INCLUDE 'TOTAL'
      INCLUDE 'NEKUSE'
C
      IF(IEL.EQ.    1.AND.ISIDE.EQ. 4.AND.IFIELD.EQ. 2)THEN
       TINF=297.594
       HC=3309.2*(ABS(TEMP-TINF))**(0.25)
      ENDIF
      IF(IEL.EQ.    1.AND.ISIDE.EQ. 5.AND.IFIELD.EQ. 2)THEN
       TINF=297.594
       HC=3309.2*(ABS(TEMP-TINF))**(0.25)
      ENDIF
      IF(IEL.EQ.    1.AND.ISIDE.EQ. 6.AND.IFIELD.EQ. 2)THEN
       IF(TIME.LT. (1*DT))THEN
        FLUX=148760000.0
       ELSEIF(TIME.GE. (1*DT))THEN
        FLUX=0.0
       ENDIF
      ENDIF
      IF(IEL.EQ.    2.AND.ISIDE.EQ. 4.AND.IFIELD.EQ. 2)THEN
       TINF=297.594
       HC=3309.2*(ABS(TEMP-TINF))**(0.25)
      ENDIF
      IF(IEL.EQ.    2.AND.ISIDE.EQ. 5.AND.IFIELD.EQ. 2)THEN
       TINF=297.594
       HC=3309.2*(ABS(TEMP-TINF))**(0.25)
      ENDIF
      IF(IEL.EQ.    2.AND.ISIDE.EQ. 6.AND.IFIELD.EQ. 2)THEN
       TINF=297.594
       HC=3309.2*(ABS(TEMP-TINF))**(0.25)
      ENDIF
      IF(IEL.EQ.    3.AND.ISIDE.EQ. 5.AND.IFIELD.EQ. 2)THEN
       TINF=297.594
       HC=3309.2*(ABS(TEMP-TINF))**(0.25)
      ENDIF
      IF(IEL.EQ.    3.AND.ISIDE.EQ. 6.AND.IFIELD.EQ. 2)THEN
       IF(TIME.GE. (5*DT).AND.TIME.LT. (6*DT))THEN
        FLUX=148760000.0
       ELSEIF(TIME.LT. (5*DT).OR.TIME.GE.(6*DT))THEN
        FLUX=0.0
       ENDIF
      ENDIF
      IF(IEL.EQ.    4.AND.ISIDE.EQ. 5.AND.IFIELD.EQ. 2)THEN
       TINF=297.594
       HC=3309.2*(ABS(TEMP-TINF))**(0.25)
      ENDIF
      IF(IEL.EQ.    4.AND.ISIDE.EQ. 6.AND.IFIELD.EQ. 2)THEN
       TINF=297.594
       HC=3309.2*(ABS(TEMP-TINF))**(0.25)
      ENDIF
      IF(IEL.EQ.    5.AND.ISIDE.EQ. 5.AND.IFIELD.EQ. 2)THEN
       TINF=297.594
       HC=3309.2*(ABS(TEMP-TINF))**(0.25)
      ENDIF
```

```
IF(IEL.EQ.    5.AND.ISIDE.EQ.  6.AND.IFIELD.EQ.  2)THEN
 IF(TIME.GE.  (1*DT).AND.TIME.LT.  (2*DT))THEN
  FLUX=148760000.0
 ELSEIF(TIME.LT.  (1*DT).OR.TIME.GE.(2*DT))THEN
  FLUX=0.0
 ENDIF
ENDIF
IF(IEL.EQ.    6.AND.ISIDE.EQ.  5.AND.IFIELD.EQ.  2)THEN
 TINF=297.594
 HC=3309.2*(ABS(TEMP-TINF))**(0.25)
ENDIF
IF(IEL.EQ.    6.AND.ISIDE.EQ.  6.AND.IFIELD.EQ.  2)THEN
 TINF=297.594
 HC=3309.2*(ABS(TEMP-TINF))**(0.25)
ENDIF
IF(IEL.EQ.    7.AND.ISIDE.EQ.  5.AND.IFIELD.EQ.  2)THEN
 TINF=297.594
 HC=3309.2*(ABS(TEMP-TINF))**(0.25)
ENDIF
IF(IEL.EQ.    7.AND.ISIDE.EQ.  6.AND.IFIELD.EQ.  2)THEN
 IF(TIME.GE.  (2*DT).AND.TIME.LT.  (3*DT))THEN
  FLUX=148760000.0
 ELSEIF(TIME.LT.  (2*DT).OR.TIME.GE.(3*DT))THEN
  FLUX=0.0
 ENDIF
ENDIF
IF(IEL.EQ.    8.AND.ISIDE.EQ.  5.AND.IFIELD.EQ.  2)THEN
 TINF=297.594
 HC=3309.2*(ABS(TEMP-TINF))**(0.25)
ENDIF
IF(IEL.EQ.    8.AND.ISIDE.EQ.  6.AND.IFIELD.EQ.  2)THEN
 TINF=297.594
 HC=3309.2*(ABS(TEMP-TINF))**(0.25)
ENDIF
IF(IEL.EQ.    9.AND.ISIDE.EQ.  5.AND.IFIELD.EQ.  2)THEN
 TINF=297.594
 HC=3309.2*(ABS(TEMP-TINF))**(0.25)
ENDIF
IF(IEL.EQ.    9.AND.ISIDE.EQ.  6.AND.IFIELD.EQ.  2)THEN
 IF(TIME.GE.  (3*DT).AND.TIME.LT.  (4*DT))THEN
  FLUX=148760000.0
 ELSEIF(TIME.LT.  (3*DT).OR.TIME.GE.(4*DT))THEN
  FLUX=0.0
 ENDIF
ENDIF
IF(IEL.EQ.   10.AND.ISIDE.EQ.  5.AND.IFIELD.EQ.  2)THEN
 TINF=297.594
 HC=3309.2*(ABS(TEMP-TINF))**(0.25)
ENDIF
IF(IEL.EQ.   10.AND.ISIDE.EQ.  6.AND.IFIELD.EQ.  2)THEN
 TINF=297.594
 HC=3309.2*(ABS(TEMP-TINF))**(0.25)
ENDIF
IF(IEL.EQ.   11.AND.ISIDE.EQ.  5.AND.IFIELD.EQ.  2)THEN
 TINF=297.594
 HC=3309.2*(ABS(TEMP-TINF))**(0.25)
ENDIF
IF(IEL.EQ.   11.AND.ISIDE.EQ.  6.AND.IFIELD.EQ.  2)THEN
 IF(TIME.GE.  (4*DT).AND.TIME.LT.  (5*DT))THEN
```

```fortran
      FLUX=148760000.0
     ELSEIF(TIME.LT. (4*DT).OR.TIME.GE.(5*DT))THEN
      FLUX=0.0
     ENDIF
    ENDIF
    IF(IEL.EQ.  12.AND.ISIDE.EQ.  5.AND.IFIELD.EQ.  2)THEN
     TINF=297.594
     HC=3309.2*(ABS(TEMP-TINF))**(0.25)
    ENDIF
    IF(IEL.EQ.  12.AND.ISIDE.EQ.  6.AND.IFIELD.EQ.  2)THEN
     TINF=297.594
     HC=3309.2*(ABS(TEMP-TINF))**(0.25)
    ENDIF
    IF(IEL.EQ.  13.AND.ISIDE.EQ.  5.AND.IFIELD.EQ.  2)THEN
     TINF=297.594
     HC=3309.2*(ABS(TEMP-TINF))**(0.25)
    ENDIF
    IF(IEL.EQ.  13.AND.ISIDE.EQ.  6.AND.IFIELD.EQ  2)THEN
     IF(TIME.GE.  (6*DT).AND.TIME.LT. (7*DT))THEN
      FLUX=148760000.0
     ELSEIF(TIME.LT. (6*DT).OR.TIME.GE.(7*DT))THEN
      FLUX=0.0
     ENDIF
    ENDIF
    IF(IEL.EQ.  14.AND.ISIDE.EQ.  5.AND.IFIELD.EQ.  2)THEN
     TINF=297.594
     HC=3309.2*(ABS(TEMP-TINF))**(0.25)
    ENDIF
    IF(IEL.EQ.  14.AND.ISIDE.EQ.  6.AND.IFIELD.EQ.  2)THEN
     TINF=297.594
     HC=3309.2*(ABS(TEMP-TINF))**(0.25)
    ENDIF
    IF(IEL.EQ.  15.AND.ISIDE.EQ.  5.AND.IFIELD.EQ.  2)THEN
     TINF=297.594
     HC=3309.2*(ABS(TEMP-TINF))**(0.25)
    ENDIF
    IF(IEL.EQ.  15.AND.ISIDE.EQ.  6.AND.IFIELD.EQ.  2)THEN
     IF(TIME.GE.  (7*DT).AND.TIME.LT. (8*DT))THEN
      FLUX=148760000.0
     ELSEIF(TIME.LT. (7*DT).OR.TIME.GE.(8*DT))THEN
      FLUX=0.0
     ENDIF
    ENDIF
    IF(IEL.EQ.  16.AND.ISIDE.EQ.  5.AND.IFIELD.EQ.  2)THEN
     TINF=297.594
     HC=3309.2*(ABS(TEMP-TINF))**(0.25)
    ENDIF
    IF(IEL.EQ.  16.AND.ISIDE.EQ.  6.AND.IFIELD.EQ.  2)THEN
     TINF=297.594
     HC=3309.2*(ABS(TEMP-TINF))**(0.25)
    ENDIF
    IF(IEL.EQ.  17.AND.ISIDE.EQ.  5.AND.IFIELD.EQ.  2)THEN
     TINF=297.594
     HC=3309.2*(ABS(TEMP-TINF))**(0.25)
    ENDIF
    IF(IEL.EQ.  17.AND.ISIDE.EQ.  6.AND.IFIELD.EQ.  2)THEN
     IF(TIME.GE.  (8*DT).AND.TIME.LT. (9*DT))THEN
      FLUX=148760000.0
     ELSEIF(TIME.LT. (8*DT).OR.TIME.GE.(9*DT))THEN
```

```
    FLUX=0.0
   ENDIF
  ENDIF
  IF(IEL.EQ.  18.AND.ISIDE.EQ.  5.AND.IFIELD.EQ.  2)THEN
   TINF=297.594
   HC=3309.2*(ABS(TEMP-TINF))**(0.25)
  ENDIF
  IF(IEL.EQ.  18.AND.ISIDE.EQ.  6.AND.IFIELD.EQ.  2)THEN
   TINF=297.594
   HC=3309.2*(ABS(TEMP-TINF))**(0.25)
  ENDIF
  IF(IEL.EQ.  19.AND.ISIDE.EQ.  2.AND.IFIELD.EQ.  2)THEN
   TINF=297.594
   HC=3309.2*(ABS(TEMP-TINF))**(0.25)
  ENDIF
  IF(IEL.EQ.  19.AND.ISIDE.EQ.  5.AND.IFIELD.EQ.  2)THEN
   TINF=297.594
   HC=3309.2*(ABS(TEMP-TINF))**(0.25)
  ENDIF
  IF(IEL.EQ.  19.AND.ISIDE.EQ.  6.AND.IFIELD.EQ.  2)THEN
   IF(TIME.GE. (9*DT).AND.TIME.LT. (10*DT))THEN
    FLUX=148760000.0
   ELSEIF(TIME.LT. (9*DT).OR.TIME.GE.(10*DT))THEN
    FLUX=0.0
   ENDIF
  ENDIF
  IF(IEL.EQ.  20.AND.ISIDE.EQ.  2.AND.IFIELD.EQ.  2)THEN
   TINF=297.594
   HC=3309.2*(ABS(TEMP-TINF))**(0.25)
  ENDIF
  IF(IEL.EQ.  20.AND.ISIDE.EQ.  5.AND.IFIELD.EQ.  2)THEN
   TINF=297.594
   HC=3309.2*(ABS(TEMP-TINF))**(0.25)
  ENDIF
  IF(IEL.EQ.  20.AND.ISIDE.EQ.  6.AND.IFIELD.EQ.  2)THEN
   TINF=297.594
   HC=3309.2*(ABS(TEMP-TINF))*(0.25)
  ENDIF
  IF(IEL.EQ.  21.AND.ISIDE.EQ.  4.AND.IFIELD.EQ.  2)THEN
   TINF=297.594
   HC=3309.2*(ABS(TEMP-TINF))**(0.25)
  ENDIF
  IF(IEL.EQ.  21.AND.ISIDE.EQ.  5.AND.IFIELD.EQ.  2)THEN
   TINF=297.594
   HC=3309.2*(ABS(TEMP-TINF))**(0.25)
  ENDIF
  IF(IEL.EQ.  21.AND.ISIDE.EQ.  6.AND.IFIELD.EQ.  2)THEN
   TINF=297.594
   HC=3309.2*(ABS(TEMP-TINF))**(0.25)
  ENDIF
  IF(IEL.EQ.  22.AND.ISIDE.EQ.  5.AND.IFIELD.EQ.  2)THEN
   TINF=297.594
   HC=3309.2*(ABS(TEMP-TINF))**(0.25)
  ENDIF
  IF(IEL.EQ.  22.AND.ISIDE.EQ.  6.AND.IFIELD.EQ.  2)THEN
   TINF=297.594
   HC=3309.2*(ABS(TEMP-TINF))**(0.25)
  ENDIF
  IF(IEL.EQ.  23.AND.ISIDE.EQ.  5.AND.IFIELD.EQ.  2)THEN
```

```
TINF=297.594
HC=3309.2*(ABS(TEMP-TINF))**(0.25)
ENDIF
IF(IEL.EQ.  23.AND.ISIDE.EQ. 6.AND.IFIELD.EQ. 2)THEN
TINF=297.594
HC=3309.2*(ABS(TEMP-TINF))**(0.25)
ENDIF
IF(IEL.EQ.  24.AND.ISIDE.EQ. 5.AND.IFIELD.EQ. 2)THEN
TINF=297.594
HC=3309.2*(ABS(TEMP-TINF))**(0.25)
ENDIF
IF(IEL.EQ.  24.AND.ISIDE.EQ. 6.AND.IFIELD.EQ. 2)THEN
TINF=297.594
HC=3309.2*(ABS(TEMP-TINF))**(0.25)
ENDIF
IF(IEL.EQ.  25.AND.ISIDE.EQ. 5.AND.IFIELD.EQ. 2)THEN
TINF=297.594
HC=3309.2*(ABS(TEMP-TINF))**(0.25)
ENDIF
IF(IEL.EQ.  25.AND.ISIDE.EQ. 6.AND.IFIELD.EQ. 2)THEN
TINF=297.594
HC=3309.2*(ABS(TEMP-TINF))**(0.25)
ENDIF
IF(IEL.EQ.  26.AND.ISIDE.EQ. 5.AND.IFIELD.EQ. 2)THEN
TINF=297.594
HC=3309.2*(ABS(TEMP-TINF))**(0.25)
ENDIF
IF(IEL.EQ.  26.AND.ISIDE.EQ. 6.AND.IFIELD.EQ. 2)THEN
TINF=297.594
HC=3309.2*(ABS(TEMP-TINF))**(0.25)
ENDIF
IF(IEL.EQ.  27.AND.ISIDE.EQ. 5.AND.IFIELD.EQ. 2)THEN
TINF=297.594
HC=3309.2*(ABS(TEMP-TINF))**(0.25)
ENDIF
IF(IEL.EQ.  27.AND.ISIDE.EQ. 6.AND.IFIELD.EQ. 2)THEN
TINF=297.594
HC=3309.2*(ABS(TEMP-TINF))**(0.25)
ENDIF
IF(IEL.EQ.  28.AND.ISIDE.EQ. 5.AND.IFIELD.EQ. 2)THEN
TINF=297.594
HC=3309.2*(ABS(TEMP-TINF))**(0.25)
ENDIF
IF(IEL.EQ.  28.AND.ISIDE.EQ. 6.AND.IFIELD.EQ. 2)THEN
TINF=297.594
HC=3309.2*(ABS(TEMP-TINF))**(0.25)
ENDIF
IF(IEL.EQ.  29.AND.ISIDE.EQ. 5.AND.IFIELD.EQ. 2)THEN
TINF=297.594
HC=3309.2*(ABS(TEMP-TINF))**(0.25)
ENDIF
IF(IEL.EQ.  29.AND.ISIDE.EQ. 6.AND.IFIELD.EQ. 2)THEN
TINF=297.594
HC=3309.2*(ABS(TEMP-TINF))**(0.25)
ENDIF
IF(IEL.EQ.  30.AND.ISIDE.EQ. 2.AND.IFIELD.EQ. 2)THEN
TINF=297.594
HC=3309.2*(ABS(TEMP-TINF))**(0.25)
ENDIF
```

```
IF(IEL.EQ.  30.AND.ISIDE.EQ. 5.AND.IFIELD.EQ. 2)THEN
 TINF=297.594
 HC=3309.2*(ABS(TEMP-TINF))**(0.25)
ENDIF
IF(IEL.EQ.  30.AND.ISIDE.EQ. 6.AND.IFIELD.EQ. 2)THEN
 TINF=297.594
 HC=3309.2*(ABS(TEMP-TINF))**(0.25)
ENDIF
IF(IEL.EQ.  31.AND.ISIDE.EQ. 3.AND.IFIELD.EQ. 2)THEN
 TINF=297.594
 HC=3309.2*(ABS(TEMP-TINF))**(0.25)
ENDIF
IF(IEL.EQ.  31.AND.ISIDE.EQ. 4.AND.IFIELD.EQ. 2)THEN
 TINF=297.594
 HC=3309.2*(ABS(TEMP-TINF))**(0.25)
ENDIF
IF(IEL.EQ.  31.AND.ISIDE.EQ. 5.AND.IFIELD.EQ. 2)THEN
 TINF=297.594
 HC=3309.2*(ABS(TEMP-TINF))**(0.25)
ENDIF
IF(IEL.EQ.  31.AND.ISIDE.EQ. 6.AND.IFIELD.EQ. 2)THEN
 TINF=297.594
 HC=3309.2*(ABS(TEMP-TINF))**(0.25)
ENDIF
IF(IEL.EQ.  32.AND.ISIDE.EQ. 3.AND.IFIELD.EQ. 2)THEN
 TINF=297.594
 HC=3309.2*(ABS(TEMP-TINF))**(0.25)
ENDIF
IF(IEL.EQ.  32.AND.ISIDE.EQ. 5.AND.IFIELD.EQ. 2)THEN
 TINF=297.594
 HC=3309.2*(ABS(TEMP-TINF))**(0.25)
ENDIF
IF(IEL.EQ.  32.AND.ISIDE.EQ. 6.AND.IFIELD.EQ. 2)THEN
 TINF=297.594
 HC=3309.2*(ABS(TEMP-TINF))**(0.25)
ENDIF
IF(IEL.EQ.  33.AND.ISIDE.EQ. 3.AND.IFIELD.EQ. 2)THEN
 TINF=297.594
 HC=3309.2*(ABS(TEMP-TINF))**(0.25)
ENDIF
IF(IEL.EQ.  33.AND.ISIDE.EQ. 5.AND.IFIELD.EQ. 2)THEN
 TINF=297.594
 HC=3309.2*(ABS(TEMP-TINF))**(0.25)
ENDIF
IF(IEL.EQ.  33.AND.ISIDE.EQ. 6.AND.IFIELD.EQ. 2)THEN
 TINF=297.594
 HC=3309.2*(ABS(TEMP-TINF))**(0.25)
ENDIF
IF(IEL.EQ.  34.AND.ISIDE.EQ. 3.AND.IFIELD.EQ. 2)THEN
 TINF=297.594
 HC=3309.2*(ABS(TEMP-TINF))**(0.25)
ENDIF
IF(IEL.EQ.  34.AND.ISIDE.EQ. 5.AND.IFIELD.EQ. 2)THEN
 TINF=297.594
 HC=3309.2*(ABS(TEMP-TINF))**(0.25)
ENDIF
IF(IEL.EQ.  34.AND.ISIDE.EQ. 6.AND.IFIELD.EQ. 2)THEN
 TINF=297.594
 HC=3309.2*(ABS(TEMP-TINF))**(0.25)
```

```
ENDIF
IF(IEL.EQ.  35.AND.ISIDE.EQ. 3.AND.IFIELD.EQ. 2)THEN
  TINF=297.594
  HC=3309.2*(ABS(TEMP-TINF))**(0.25)
ENDIF
IF(IEL.EQ.  35.AND.ISIDE.EQ. 5.AND.IFIELD.EQ. 2)THEN
  TINF=297.594
  HC=3309.2*(ABS(TEMP-TINF))**(0.25)
ENDIF
IF(IEL.EQ.  35.AND.ISIDE.EQ. 6.AND.IFIELD.EQ. 2)THEN
  TINF=297.594
  HC=3309.2*(ABS(TEMP-TINF))**(0.25)
ENDIF
IF(IEL.EQ.  36.AND.ISIDE.EQ. 3.AND.IFIELD.EQ. 2)THEN
  TINF=297.594
  HC=3309.2*(ABS(TEMP-TINF))**(0.25)
ENDIF
IF(IEL.EQ.  36.AND.ISIDE.EQ. 5.AND.IFIELD.EQ. 2)THEN
  TINF=297.594
  HC=3309.2*(ABS(TEMP-TINF))**(0.25)
ENDIF
IF(IEL.EQ.  36.AND.ISIDE.EQ. 6.AND.IFIELD.EQ. 2)THEN
  TINF=297.594
  HC=3309.2*(ABS(TEMP-TINF))**(0.25)
ENDIF
IF(IEL.EQ.  37.AND.ISIDE.EQ. 3.AND.IFIELD.EQ. 2)THEN
  TINF=297.594
  HC=3309.2*(ABS(TEMP-TINF))**(0.25)
ENDIF
IF(IEL.EQ.  37.AND.ISIDE.EQ. 5.AND.IFIELD.EQ. 2)THEN
  TINF=297.594
  HC=3309.2*(ABS(TEMP-TINF))**(0.25)
ENDIF
IF(IEL.EQ.  37.AND.ISIDE.EQ. 6.AND.IFIELD.EQ. 2)THEN
  TINF=297.594
  HC=3309.2*(ABS(TEMP-TINF))**(0.25)
ENDIF
IF(IEL.EQ.  38.AND.ISIDE.EQ. 3.AND.IFIELD.EQ. 2)THEN
  TINF=297.594
  HC=3309.2*(ABS(TEMP-TINF))**(0.25)
ENDIF
IF(IEL.EQ.  38.AND.ISIDE.EQ. 5.AND.IFIELD.EQ. 2)THEN
  TINF=297.594
  HC=3309.2*(ABS(TEMP-TINF))**(0.25)
ENDIF
IF(IEL.EQ.  38.AND.ISIDE.EQ. 6.AND.IFIELD.EQ. 2)THEN
  TINF=297.594
  HC=3309.2*(ABS(TEMP-TINF))**(0.25)
ENDIF
IF(IEL.EQ.  39.AND.ISIDE.EQ. 3.AND.IFIELD.EQ. 2)THEN
  TINF=297.594
  HC=3309.2*(ABS(TEMP-TINF))**(0.25)
ENDIF
IF(IEL.EQ.  39.AND.ISIDE.EQ. 5.AND.IFIELD.EQ. 2)THEN
  TINF=297.594
  HC=3309.2*(ABS(TEMP-TINF))**(0.25)
ENDIF
IF(IEL.EQ.  39.AND.ISIDE.EQ. 6.AND.IFIELD.EQ. 2)THEN
  TINF=297.594
```

```
            HC=3309.2*(ABS(TEMP-TINF))**(0.25)
      ENDIF
      IF(IEL.EQ.   40.AND.ISIDE.EQ.  2.AND.IFIELD.EQ.  2)THEN
       TINF=297.594
       HC=3309.2*(ABS(TEMP-TINF))**(0.25)
      ENDIF
      IF(IEL.EQ.   40.AND.ISIDE.EQ.  3.AND.IFIELD.EQ.  2)THEN
       TINF=297.594
       HC=3309.2*(ABS(TEMP-TINF))**(0.25)
      ENDIF
      IF(IEL.EQ.   40.AND.ISIDE.EQ.  5.AND.IFIELD.EQ.  2)THEN
       TINF=297.594
       HC=3309.2*(ABS(TEMP-TINF))**(0.25)
      ENDIF
      IF(IEL.EQ.   40.AND.ISIDE.EQ.  6.AND.IFIELD.EQ.  2)THEN
       TINF=297.594
       HC=3309.2*(ABS(TEMP-TINF))**(0.25)
      ENDIF
      RETURN
      END
C
      SUBROUTINE USERIC (IX,IY,IZ,IEL)
      INCLUDE 'SIZE'
      INCLUDE 'TSTEP'
C     INCLUDE 'TOTAL'
      INCLUDE 'NEKUSE'
       IF (IFIELD.EQ.1) THEN
         UX=0
         UY=0
         UZ=0
C Default
      ELSE IF(IFIELD.EQ.            2)THEN
       TEMP=297.594
      ENDIF
      RETURN
       END
```